ABSTRACT

CHEN, CHEN. Preparation and Characterization of Electrospun Polyvinylidene fluoride (PVDF) Membrane and Electrospun PVDF Coated Polypropylene (PP) Nonwoven Membranes as Lithium-ion Battery Separators. (Under the direction of Dr. Xiangwu Zhang).

Currently, lithium-ion batteries are widely used in many applications such as portable laptops and cellphones due to their appropriate operating voltage, high energy and power density, low self-discharge rate, no memory effect, and long cycle life. Separator, as a composing part of lithium-ion batteries, plays an important role in determining the battery performance and safety. The poor wettability and low porosity of current polyolefin separators limit the performance of lithium-ion batteries.

In this study, electrospinning was used to produce polyvinylidene fluoride (PVDF) nanofiber membranes. These PVDF nanofiber membranes showed higher electrolyte uptake capacity and ionic conductivity than traditional polyolefin separators. In addition to using PVDF nanofiber membranes directly as the separator, PVDF nanofibers were also deposited onto the both sides of polypropylene (PP) nonwoven substrates to obtain novel composite membranes. The electrospun PVDF-coated PP membranes also exhibited good electrolyte uptake capacity, ionic conductivity, and charge-discharge performance.

Preparation and Characterization of Electrospun PVDF Membranes and Electrospun PVDF Coated PP Nonwoven Membranes as Lithium-ion Battery Separator

by
Chen Chen

A thesis submitted to the Graduate Faculty of
North Carolina State University
in partial fulfillment of the
requirements for the degree of
Master of Science

Textile Engineering

Raleigh, North Carolina

2013

APPROVED BY:

_____
Dr. Xiangwu Zhang
Chair of Advisory Committee

_____ _____
Dr. Philip Bradford Dr. Wendy Krause

DEDICATION

This thesis is dedicated to my parents for their support through my life.

BIOGRAPHY

Chen Chen was born in PuYang City in HeNan Province, China. He majored in Textile Engineering at Donghua University, China from September 2008 to June 2011 and obtained his Bachelor of Engineering degree in June 2012. In August 2011, he came to North Carolina State University as an exchange student under the 3 + X program to pursue his Master of Science degree. He joined Dr. Xiangwu Zhang's group in December 2011. After completing the Master program, he plans to pursue a Ph.D. degree.

ACKNOWLEDGMENTS

I would like to thank first and foremost my advisor, Dr. Xiangwu Zhang, for offering the opportunity of my Master study and his support and guidance throughout my research. I would like to express my appreciation to my committee members: Dr. Wendy Krause and Dr. Philip Bradford for their interest in my work.

I would like to thank Mr. Chuck Mooney for his help during the SEM analysis.

I greatly appreciate Kun Fu, Shuli Li, Yao Lu and Meltem Yanilmaz for their sincere help and discussion in my study. Also, I want to thank all the other group members for their help.

Last but not least, I would like to express my appreciation to my parents for their love and encouragement for my life. I would like to thank my friends for their love and support.

TABLE OF CONTENTS

LIST OF TABLES viii

LIST OF FIGURES ix

Chapter 1 Introduction 1

Chapter 2 Literature Review 3

2.1 Lithium-ion Batteries 3

2.1.1 Development of batteries 3

2.1.2 Development of lithium-ion batteries 6

2.1.3 Battery structures and electrochemical principles 8

2.1.4 Components of lithium ion batteries 10

2.1.4.1 Cathode 10

2.1.4.2 Anode 14

2.1.4.3 Electrolyte 18

2.1.4.4 Separator 20

2.2 Electrospinning and Electrospun Nanofibers 26

2.2.1 Overview of Electrospinning 26

2.2.2 Influencing parameters in electrospinning 28

Chapter 3 Research Objectives 34

3.1 Fabrication of Polyvinylidene Fluoride (PVdF) Nanofiber Membranes through Electrospinning for Use as Separators in Lithium-ion Batteries. 34

3.2 Fabrication of Nanofiber-coated Nonwoven Polypropylene Composite through Electrospinning and Hot-pressing Treatment for Use as Separators in Lithium-ion Batteries. 35

Chapter 4 Electrospun PVDF Nanofiber Membrane for Lithium-ion Battery Separators 36

Abstract 36

4.1 Introduction 38
4.2 Experimental 39
4.2.1 Materials 39
4.2.2 Preparation of nanofiber separators 40
4.2.3 Structure characterization and property measurements 40
4.3 Results and Discussion 43
4.3.1 SEM 43
4.3.2 Tensile properties 47
4.3.3 Electrolyte Uptake 48
4.3.4 Ionic Conductivity 50
4.3.5 Electrochemical Stability Window 53
4.3.6 Battery Performance 56
4.4 Conclusion 57
Chapter 5 Electrospun PVDF-Coated Nonwoven Polypropylene for Lithium-ion Battery Separator 59
Abstract 59
5.1 Introduction 60
5.2 Experimental 62
5.2.1 Material 62
5.2.2 Preparation of Electrospun PVDF-coated PP Nonwoven membrane 62
5.2.3 Structure characterization and property measurements 64
5.3 Result and Discussion 66
5.3.1 SEM images 66
5.3.2 Tensile properties 68

5.3.3 Electrolyte Uptake 70

5.3.4 Ionic Conductivity 72

5.3.5 Electrochemical Stability Window 73

5.3.6 Cell Performance 75

5.3.7 Raman spectra 76

5.4 Conclusion 77

Chapter 6 Conclusion 79

Chapter 7 Recommendation work 82

References 83

LIST OF TABLES

Table 2.1 Key parameters for 1 Amphour secondary batteries 8

Table 2.2 Behaviour of cation-conducting electrolyte materials 19

Table 2.3 Major manufacturers of lithium-ion battery separators along with their typical products 22

Table 2.4 General requirements for lithium-ion battery separator 24

Table 4.1 Average tensile strength, modulus, and strain-at-break of un-pressed and hot-pressed electrospun PVDF membranes. 47

Table 5.1 Average tensile strength, modulus, and strain-at-break of PP nonwoven fabric, electrospun PVDF membrane (hot-pressed), and electrospun PVDF-coated PP nonwoven membrane 69

LIST OF FIGURES

Figure 2.1 Gravimetric power and energy densities for different rechargeable batteries. Most of these systems are currently being investigated for grid storage applications.....5

Figure 2.2 Market prospect of power storage (NAS: Na–S battery, Pumped Hydro: pumpedstorage hydroelectricity, CAES: compressed air energy storage).....6

Figure 2. 3 Schematic drawing showing the shape and components of various Li-ion battery configurations. a, Cylindrical; b, coin; c, prismatic; and d, thin and flat.....9

Figure 2.4 Principle of lithium-ion batteries.....10

Figure 2.5 Layered structure of LiTiS2, LiVSe2, LiCoO2, LiNiO2, and LiNixMnxCo1-2xO2, showing the lithium ions between the transition-metal oxide/sulfide sheets. The actual stacking of the metal oxide sheets depends on the transition metal and the anion.....12

Figure 2.6 Crystal structure of spinel LiM2O4 (blue: transition metal ions; red: Li ions) 13

Figure 2.7 Crystal structure of (a) LiFePO4 and (b) order structure of olivine stack.....14

Figure 2.9 Gravimetric and volumetric capacities for selected alloying reactions. Capacities for graphite are given as references.....18

Figure 2.10 Scanning electron micrographs of Celgard separators used in lithium-ion batteries: (a) 2400 (PP), (b) 2500 (PP), and (c) 2730 (PE).....26

Figure 2. 11 A typical electrospinning set-up using a grounded static collector.....27

Figure 2.12 Concentration effect on microstructures of electrospun poly(D,L-lactic acid) nanofibers at voltage of 20 kV, feeding rate of 20 ml/min, and concentration of (A) 20 wt%; (B) 25 wt%; (C) 30 wt% and (D) 35 wt%. 29

Figure 2.13 Effect of voltage on the morphology of nanofibers jet through the air. Electrospun from 3.85 wt% poly(ethylene oxide) in water. Electric field is 0.4 kV/cm. The horizontal edge of each of the figures is 20 microns long.....31

Figure 2.14 FESEM micrographs of 190 000 g/mol PS/tetrahydrofuran fibers electrospun under varying humidity: (a) <25%, (b) 31-38%, (c) 40-45%, (d) 50-59%, (e) 60-72% [74]. 33

Figure 4.1 SEM images of electrospun PVDF membranes prepared with different voltages: (A, B) 10kV, (C, D) 15kV, and (E, F) 20kV. 44

Figure 4.2 Diameter distribution of electrospun PVDF fibers prepared with different voltages: (A) 10kV, (B) 15kV, and (C) 20kV. 45

Figure 4.3 SEM images of electrospun PVDF membranes (A) before, and (B) after hot-press. 46

Figure 4.4 Electrolyte uptakes as a function of time for Celgard membrane and PVDF membranes prepared under different applied voltages: 10kV, 15kV and 20kV. 49

Figure 4.5 Electrolyte uptakes as a function of time for Celgard membrane and un-pressed and hot-pressed electrospun PVDF membranes. 50

Figure 4.6 Ionic conductivities of liquid electrolyte-soaked Celgard membrane and electrospun PVDF membrane under different voltages: 10kV, 15kV, 20kV and as a function of temperature. 52

Figure 4.7 Ionic conductivities of Celgard membrane, and un-pressed and hot-pressed electrospun PVDF membranes as a function of temperature. 53

Figure 4.8 Electrochemical stability windows of Celgard and electrospun PVDF membranes with different applied voltages: 10kV, 15kV, 20kV. 54

Figure 4.9 Electrochemical stability windows of Celgard, and un-pressed and hot-pressed electrospun PVDF membranes. 55

Figure 4.10 Charge-discharge curves of Li/$LiFePO_4$ cells containing: (A) Celgard, (B) un-pressed electrospun PVDF, (C) hot-pressed electrospun PVDF membranes. 56

Figure 4.11 Cycle performance of Li/$LiFePO_4$ cells with Celgard membrane, un-pressed electrospun PVDF, membrane and hot-pressed electrospun PVDF membranes. 57

Figure 5.1 Schematic of the experimental process. 63

Figure 5.2 SEM images of PP nonwoven substrate. 67

Figure 5.3 SEM images of electrospun PVDF-coated PP nonwoven membranes. 68

Figure 5.4 Electrolyte uptakes as a function of time for Celgard, PP nonwoven, electrospun PVDF, and electrospun PVDF-coated PP nonwoven. 71

Figure 5.5 Ionic conductivities of liquid electrolyte-soaked membranes at various temperatures. 72

Figure 5.6 Electrochemical stability windows of liquid electrolyte-soaked Celgard, PP non-woven fabric, electrospun PVDF-coated PP nonwoven membranes. 74

Figure 5.7 Charge-discharge curves of Li/$LiFePO_4$ cells containing: (A) Celgard, (B) electrospun PVDF, and (C) electrospun PVDF-coated PP nonwoven membrane.....75

Figure 5.8 Cycle performance of Li/LiFePO4 cells containing Celgard, electrospun PVDF membrane, and electrospun PVDF-coated PP nonwoven membranes.....76

Figure 5.9 Raman spectra of electrospun PVDF-coated PP nonwoven membrane before and after cycling.....77

Chapter 1 Introduction

With increasing demand for energy, energy conversion and storage are becoming more important than ever before. The use of fossil fuel has been proved harmful to our environment. Renewable energy sources like solar, wind energy are promising, but need to be used with energy storage devices due to their low efficiency and high fluctuation in weather condition and so on. Battery, as a device that stores electrical energy in a form of chemical energy to electric energy, is one of the most promising and appropriate forms of energy storage.

Among various battery types, lithium-ion battery has attracted great attention for its great advantages such as high energy and power density, appropriate operating potential, good rate capability, no memory effect, etc.

As an important comprising part of lithium-ion battery, separator is a porous polymer membrane sandwiched between the anode and the cathode to prevent direct contact of two electrodes. Currently, the membrane separators used for commercial lithium-ion batteries are mainly made of microporous polyolefin which has relatively low porosity and poor wettability. These disadvantages limit the performance of lithium-ion batteries. Therefore, the development of new types of separators is in urgent need. The motivation of this study is to develop the nanofiber-based separators with high wettability and porosity through electrospinning.

In this study, polyvinylidene fluoride (PVDF) nanofiber membranes were prepared through electrospinning under three different applied voltages and followed by hot-press

treatment. Composite membranes were also prepared by depositing electrospun PVDF onto both sides of polypropylene nonwoven fabrics. The structure, morphology, tensile properties, electrolyte uptake, ionic conductivity, electrochemical stability window, and electrochemical performance of these two membrane separators were evaluated.

Chapter 2 Literature Review

2.1 Lithium-ion Batteries

2.1.1 Development of batteries

Since the utilization of fire in the ancient times by our ancestors which is also an extraordinary milestone in the development of human civilization, people truly began to convert one kind of energy to another one and took advantage of it. However, it took human beings a very long time to touch the area of electricity since the gift of Prometheus was presented to people millions of years ago. Before the electricity, which is one of the most important achievements in the history, was fully known and utilized by people, various kinds of fossil fuel were mined and utilized to provide energy for different kinds of uses. People's life has been changed tremendously after electricity was brought to our daily life [1]. Generally speaking, battery is a device that is able to store electricity in the form of chemical energy. As an early start of developing batteries, Alessandro Volta invented the electric piles at the end of the eighteenth century in Italy and that was inspired by the observation that the legs of frogs would twitch when touched by two different kinds of metals at the same time [1, 2]. After that, lead-acid batteries, which is the oldest rechargeable battery, was inverted in 1859 by Gaston Plante, and after some developments like the coating methods for both sides of lead plates by Camille Faure and so on, lead-acid batteries have been widely used in the automobile starter motors which requires high current [1, 4]. With the higher price of fossil fuels and the indisputable fact that we are approaching the limited availability of the fossil fuels, battery technique has

gained great accomplishment in the last decades [5]. Especially in recent years, the greenhouse effect rising from the massive emission of carbon dioxide into the atmosphere has become stimulated the need for renewable energy and therefore battery and related techniques has obtained a rapid development [5, 6]. In spite of other energy resources like the nuclear energy and solar energy, battery takes the advantage over them at once for the reasons that nuclear energy has been proved to have great potential to take place of fossil fuels, however, what happened in Chernobyl has given us a startling lesson about the danger of nuclear energy. In terms of solar energy, it is still in the development of infancy stage and the transfer efficiency of its limited applications is still not able to satisfy our increasing need for energy.

Batteries can be classified into two kinds, the primary batteries which are disposable, and secondary batteries which are rechargeable [4]. Although some primary batteries can be charged under certain condition, and the ability to be charged is limited [7].

After the lead-acid batteries, Jungner invented the nickel-iron batteries the early 20^{th} century and the durability of the nickel-iron batteries is so good that it can keep a good condition in spite of overcharge, overdischarge and short circuiting [8, 9]. Among various secondary batteries, lithium ion batteries have its irreplaceable advantages, for example the lithium ion batteries have the highest energy densities per unit, as shown in Figure 1 [10]. Besides, due to the relatively small ionic radius of lithium, the diffusion properties of lithium ion batteries is very good and its low redox potential also enables high-output voltages which lead to high-energy densities [11]. Other advantages including long cycle

life and high rate capability of lithium-ion batteries, as a result, make lithium-ion batteries occupy a very important place in the battery market.

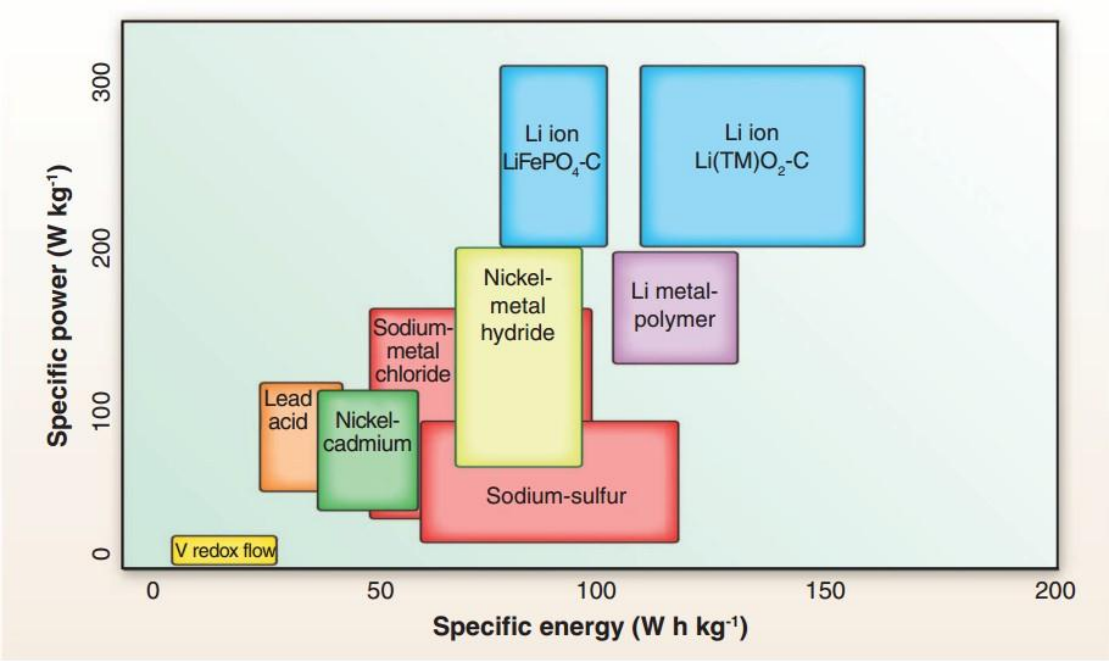

Figure 2.1 Gravimetric power and energy densities for different rechargeable batteries. Most of these systems are currently being investigated for grid storage applications [10].

As it is shown in Figure 2.2, the market demand for lithium-ion batteries is expected to increase rapidly in the next decade.

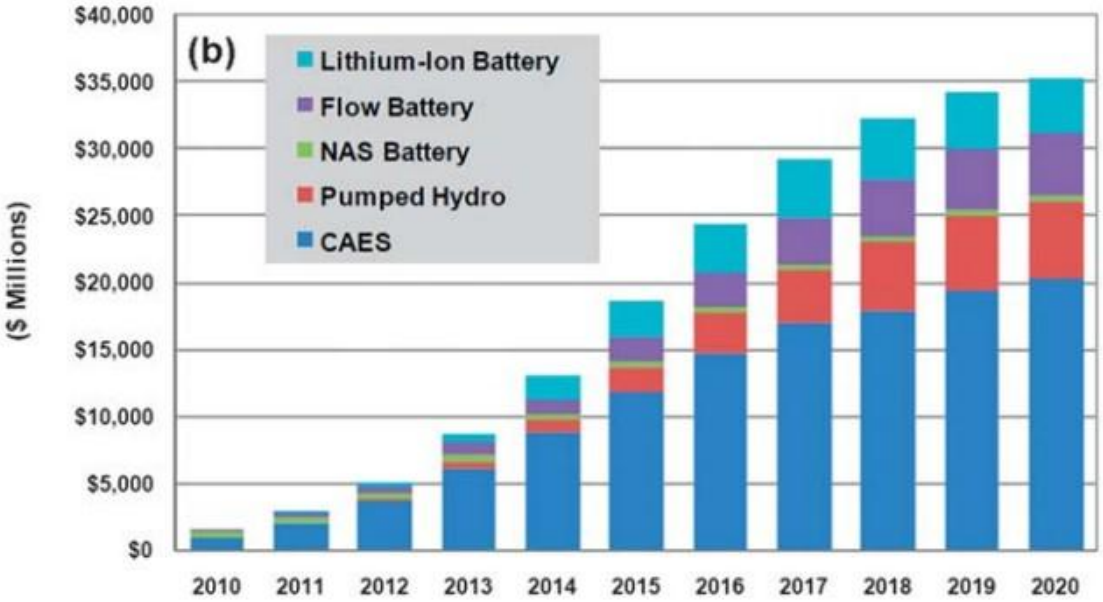

Figure 2.2 Market prospect of power storage (NAS: Na–S battery, Pumped Hydro: pumpedstorage hydroelectricity, CAES: compressed air energy storage) [12].

2.1.2 Development of lithium-ion batteries

Initially, the reason that people select lithium as the battery anode is based on the fact that lithium is the most electronegative (–3.04 V versus standard hydrogen electrode), at the same time, and the lightest metal in the periodic table of chemical element, which provide lithium with very high energy density [13]. Prior to lithium-ion batteries, the primary batteries with lithium metal as the anode have been widely used in some applications with outstanding advantages like high voltage, a high energy density, a low self-discharge rate, and wide operation temperature range compared with conventional primary batteries [14]. However, using lithium metal as anode could cause explosion hazards [13, 14]. So researchers came up with some ways to solve this safety problems, for example, replacing the lithium metal with a second insertion material or applying dry polymer electrolyte for

the batteries instead of liquid electrolyte [13]. Since 1970s, the rapid development of portable electric devices like notebook computers, cellphones and so on enable lithium ion batteries a good development period. The first batch of lithium-ion batteries was commercialized by SONY in 1991 which decreased the size and weight of portable electric devices significantly [15]. In addition to being the power source for portable electric devices, lithium-ion batteries now have begun to satisfy the demands for hybrid electric vehicles. In 2007, 1600 MMT of CO_2 emissions is attributed to the waste gas from vehicles [16, 17]. Many efforts have been made to replace traditional vehicles with hybrid or electric ones to decrease the CO_2 emissions which will have significant impact on the environmental protection. From Table 1, it is seen that the advantages of lithium ion batteries over other two kinds of batteries which are both used in hybrid electric vehicles [16]. So a lot of researches nowadays focus on the application of lithium ion batteries on hybrid electrical vehicles which lead to emerge of many new materials for the lithium ion materials.

Table 2.1 Key parameters for 1 Amphour secondary batteries [16].

	Lead acid	Nickel metal hydride	Lithium ion
Specific energy	20-35 Wh/kg	~65 Wh/kg	90 Wh/kg
Energy density	54-95 Wh/L	~150 Wh/L	153 Wh/L
Specific power	~250 W/kg	200 W/kg	300 W/kg
Nominal cell voltage	2 V	1.2 V	3.5 V
Internal resistance	~.022 Ω per cell	~.06 Ω per cell	~.2 Ω per cell
Self-discharge	~2% a day	~5% a day	~10% a month
Charge time	8h (90% in 1h possible)	1h (60% in 20min possible)	2-3h

2.1.3 Battery structures and electrochemical principles

In general, a lithium-ion battery consists of four main components which respectively are negative electrode, positive electrode, separator, and electrolyte. As shown in the

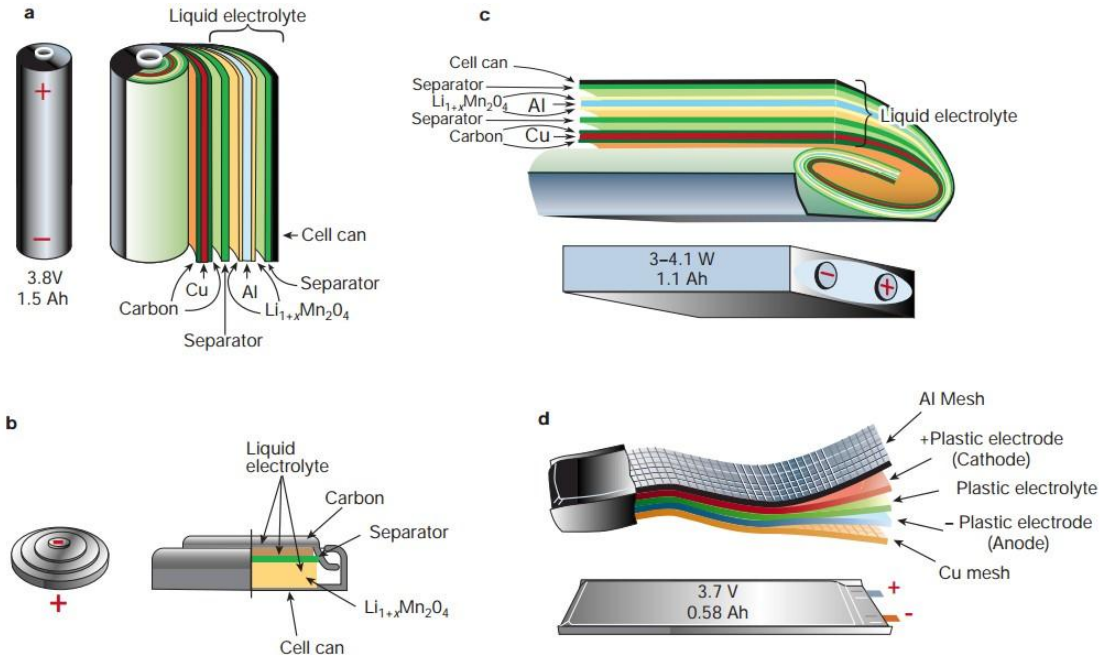

Figure 2. 1 Schematic drawing showing the shape and components of various Li-ion battery configurations. a, Cylindrical; b, coin; c, prismatic; and d, thin and flat [13].

In terms of the electrochemical principles of lithium ion batteries, the intercalation compounds such as $LiCoO_2$, is used as the positive electrode and carbonaceous materials such as graphite itself, is employed as the negative electrode [14, 18]. Both materials of anode and cathode must permit free migration of lithium ions [19]. The general electrochemical reactions between the anode and the cathode during charge and discharge are described as follows [18]:

Negative electrode:

$$C + x\ Li^+ + x\ e^- \leftrightarrow Li_x\ C \qquad (2.1)$$

Positive electrode:

$$LiCoO_2 \leftrightarrow Li1_{-x}CoO_2 + xLi^+ + xe^- \qquad (2.2)$$

Overall reaction:

$$C+LiCoO_2 \leftrightarrow Li_x C + Li_{1-x}CoO_2 \quad (2.3)$$

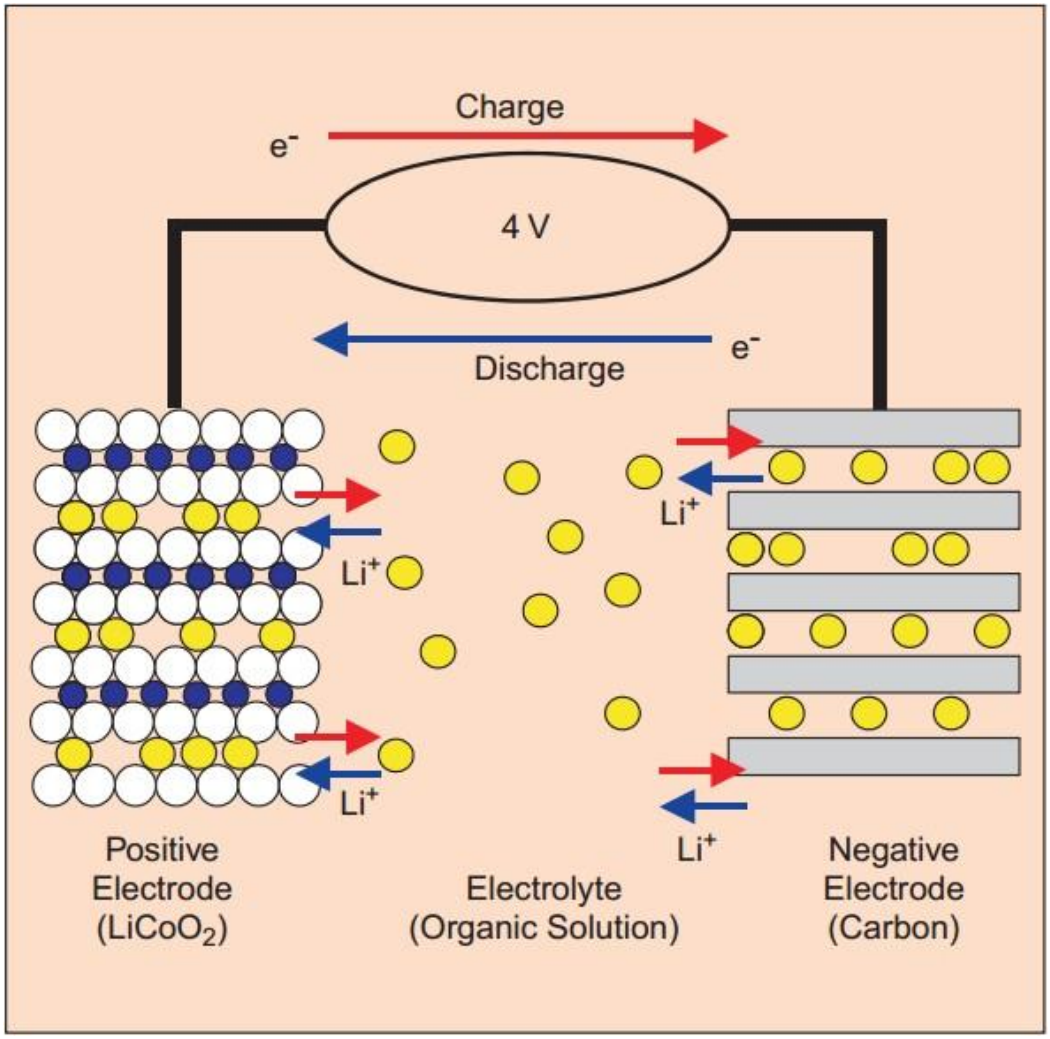

Figure 2.4 Principle of lithium-ion batteries [18].

As it is shown in the Figure 2.4, the trivalent cobalt ions in $LiCoO_2$ are oxidized during charging at the positive electrode, while the lithium ions in the solution are intercalated between the layers of graphite at the negative electrode [18].

2.1.4 Components of lithium ion batteries

2.1.4.1 Cathode

The cathode is actually an electrode where electric current flows out, during charging process by producing the Li^+ and e^-. Technically speaking, one of the most challenging parts in improving lithium-ion battery performance is to find a suitable cathode material for the battery. As an effective lithium ion cathode material, there some requirements. At first, the material must have an intercalation-type reaction which means that the host chemical structure of the cathode should not change when lithium is introduced [20]. Based on the amount of the open structure available in the material, the cathode material can be roughly classified into two types [20]. For the first type, the compound forms layer structures packed by close anion lattice such as $LiCoO_2$, $LiNi_{1-x}Co_xO_2$, and $LiNi_xMnxCo_{1-2x}O_2$, as shown in Figure 2.5, and compared with the first type, representative of the second type of cathode material like $LiFePO_4$ has more open structure which, because of the absence of core compact lattice, leads to less energy storage per unit of volume, however, is less expensive [20, 21].

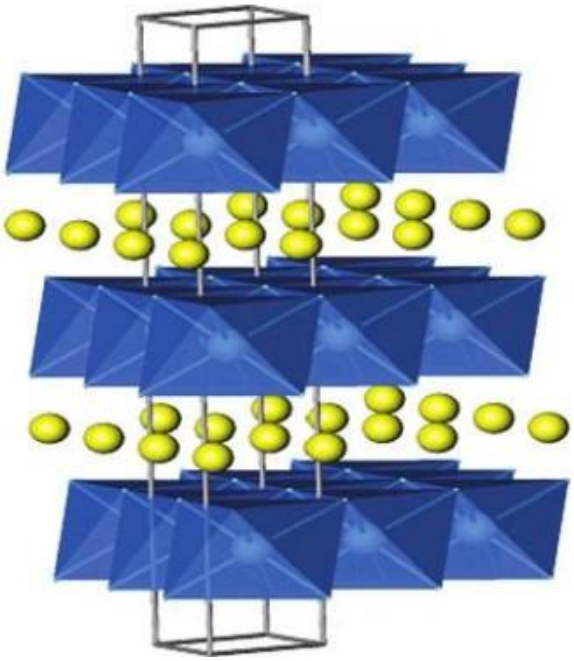

Figure 2.5 Layered structure of LiTiS2, LiVSe2, LiCoO2, LiNiO2, and LiNixMnxCo1-2xO2, showing the lithium ions between the transition-metal oxide/sulfide sheets. The actual stacking of the metal oxide sheets depends on the transition metal and the anion [20].

$LiCoO_2$ was first utilized as a cathode material by John Goodenough in 1980 [22] and also was combined with the carbon anode by SONY to produce the first batch of commercialized lithium ion battery [25]. As one of the most widespread cathode material, $LiCoO_2$ can be cycled more than 500 times with 80–90% capacity retention resulting from its excellent structural stability with a very high potential [23]. $LiCoO_2$ forms the α-$NaFeO_2$ structure which allow the lithiation and delithiation to occur between planes of lithium ions [24]. However, the specific capacity of $LiCoO_2$ is only around 130 mAh/g which is much lower than the theoretical capacity, and the reason for that is only around 0.5 Li/Co can be cycled successfully without resulting in capacity loss [20]. In addition, in spite of the fact that $LiCoO_2$ is in a dominant position in the lithium ion battery market,

the limitation of cobalt resource leads to a very high price [20-26].

$LiMn_2O_4$ is another promising material with spinel-type structure as shown in Figure 2.6 which is closely related to α-$NaFeO_2$ layer structure, and the only difference is the distribution of the cations [20, 26-27].

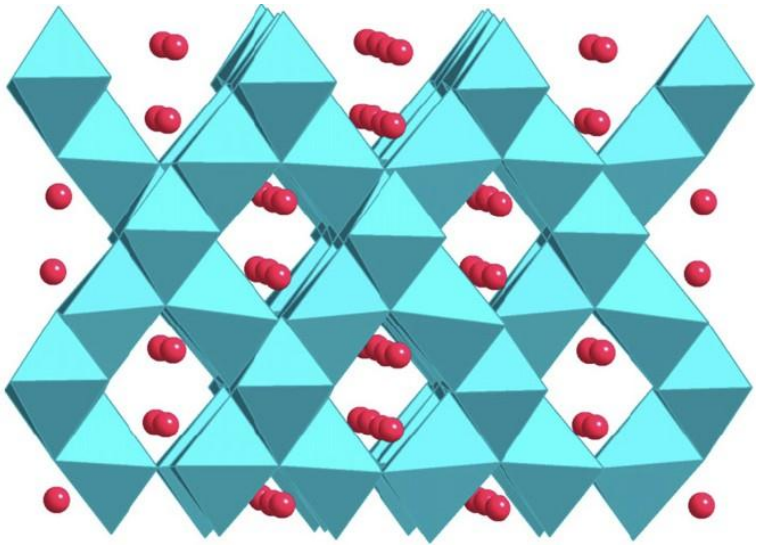

Figure 2.6 Crystal structure of spinel LiM2O4 (blue: transition metal ions; red: Li ions) [26].

Compared with $LiCoO_2$, $LiMn_2O_4$ is low-cost, environmentally friendly, and abundant in the nature. However, because of the dissolution of manganese, which occurs at >4.4V Li/Li^+ potential, $LiMn_2O_4$ has serious capacity fading problem [28].

Another kind of cathode material is olivine compounds $LiMPO_4$, and the most representative one is $LiFePO_4$ which attracts lots of attention due to its excellent electrochemical properties, good thermal stability, and low cost [26].

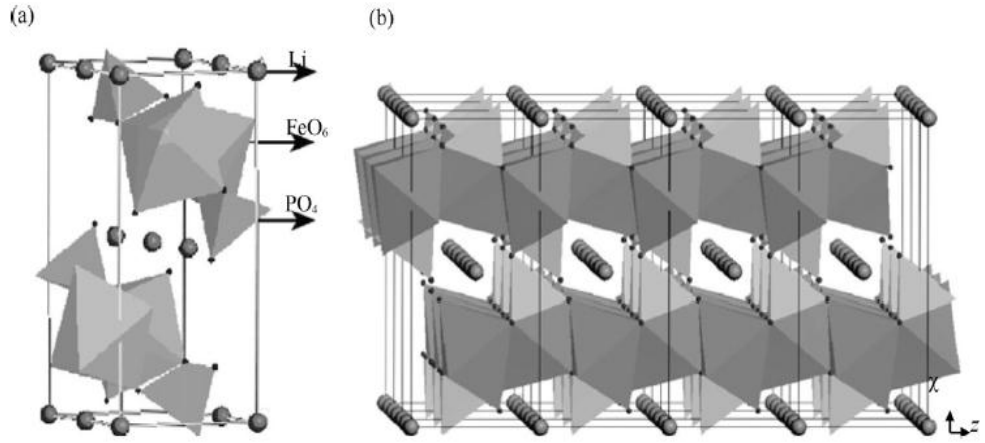

Figure 2.7 Crystal structure of (a) LiFePO4 and (b) order structure of olivine stack [29].

In $LiFePO_4$, a closly-packed hexagonal framework is formed with Li and Fe are located in octahedral sites and P is located in tetrahedral sites [30]. $LiFeO_4$ has a relatively high theoretical capacity of 170 mAh g^{-1}, however, this material has low intrinsic electronic conductivity and low ion diffusion rate of Li^+ [30-33].

Various methods have been used to produce $LiFePO_4$ such as solid-state reaction, sol–gel method, microwave processes, hydrothermal synthesis and so on [33]. According to different producing methods, the discharge capacities of the $LiFePO_4$/C are different [34, 35]. For example, Dong et al. [34] prepared $LiFePO_4$ and C compositewith a discharge specific capacity of 157mAh g^{-1} at 0.1 C using the solid-state method and Park et al. [35] got a discharge specific capacity of 151mAh g^{-1} at 0.1 C with the microwave processing. Currently, the most common method that is utilized to produce $LiFePO_4$ is still the high temperature solid-state reaction.

2.1.4.2 Anode

Anode is different in the varieties of available material from cathode which is mostly

limited to intercalation/insertion compounds, and the materials that can satisfy the requirements for lithium ion batteries anodes include carbonaceous material like graphite. Li alloys and metal oxides and so on [36, 37].

Carbonaceous material dominates the commercial lithium ion batteries since SONY succeeded in making the first patch of commercialized lithium ion batteries with $C/LiCoO_2$ in the early 1990s [15]. One of the most important reasons that makes carbonaceous material take place of lithium metal which has a theoretical capacity of 3860 mAh g^{-1}, much higher that 372 mAh g^{-1} for LiC_6, is that there are safety concerns because of the dendrite formation on the surface of lithium metal in the process of charge/discharge [36, 38]. The performance of carbonaceous material really depends on the morphology and structure of the material [36]. For example, hard carbon shows a capacity of 200–600 mA h g^{-1}, and that's because each layered graphene can absorb lithium ions on both sides at higher voltage before filling the micropores in hard carbons with lithium ions at relatively lower voltage [36, 39]. However, in spite of a very high reversible Li-storage capacity for soft carbons, it will process a serious voltage hysteresis during delithiation [39]. There are some mechanisms proposed to explain the structural influencing parameters of carbonaceous materials like stacking fidelity and defect of the basal planes [38]. Some disadvantages of carbonaceous anode materials like graphite still exist like lower theoretical capacity (372 $mAhg^{-1}$) compared to other possible anode materials, such as the lithium alloys of silicon or tin [40]. So people are still seeking novel ways to improve the performance of anode materials. Some researchers found mild

oxidation of graphite with O_2 could lead to an increase in the electrochemical performance [41]. The mechanism of this process is attributed to the formation of nanochannels and /or micropores and the dense layer of oxides [41]. Forming composites with metal and metal oxides is another way people have explored to enhance the performance of carbonaceous anode materials [37]. Mixing nanosized Ni with graphite demonstrates a significant improvement in charge-discharge performance, coulombic efficiency and cycling behavior [37].

However, the maximum available capacity of carbon anode is limited by the number vacant sites in the structure [36]. So researchers are still seeking alternative anode materials.

In 1995, researchers in Fuji Film Co. succeeded in using tin-based composite oxides as anode active materials which showed 500–600mA h g^{-1} reversible capacities [42]. A basic formula for the material is SnM_xO_y, and the M stands for a group of glass-forming metallic elements with an equal or higher number of total stoichiometric number than tin ($x \geq 1$) [42]. The storage mechanism of tin-based oxides occurs by a two-step reaction [36]:

$$2Li + SnO \rightarrow Li_2O + Sn \quad (2.4)$$

$$4.4Li + Sn \leftrightarrow Li_{22}Sn_5 \quad (2.5)$$

There are also some developed structure of tin-based anodes like hollow SnO_2 microsphere for the lithium-ion batteries, which exhibits very high discharge capacities and higher coulombic efficiency [43].

Another promising kind of material that can be used to produce lithium ion battery anode is the nanosized alloy. Many metals and alloys have a significant ability to store Li by forming Li alloys which leads to a very high storage capacity, for example, $Li_{4.4}Si$, which corresponds to a Li storage capacity as high as 4200 mA h g^{-1} [36]. During charge/discharge process, the dimensional stability of host material plays an important role in the cycle performance, however, the expansion and contraction during this process will happen which is a serious barrier and often leads to instability of the electrode material and poor cyclic performance [36, 44]. It has been proved that nanosized particles such as $Sn(SnSb)_{0.14}$ (200nm) had a higher endurance to volume change [45]. Among all the alloy materials, Si is a very good candidate to increase the capacity of the anode. At room temperature, the Si nanoparticles show a reversible capacity to 1700mA h g^{-1} [46]. However, there is a drawback about Si nanoparticles. After one cycle, delithiation will keep Si atoms in a dangling bond state with high energy, then serious agglomeration occurs [47].

The last but not the latest attractive candidate for anode material is transition metal oxides. In 2000, Poizot et al. reported that the transition metal oxides has the ability to store Li reversibly through the reaction: $Li + TMO \rightarrow Li_2O + TM$ where TM is Co, Fe, Ni, Cr, Mn and Cu, and the gravimetric and volumetric capacities of different alloy have been shown in the Figure 2.8 [36, 48, 51]. Cr_2O_3 and MnO, with a high lithiation capacity but relatively low thermodynamic equilibrium voltage (1.085 and 1.032 V vs Li/Li^+), are suitable for being anode material, because in order to approach the theoretical lithiation

capacity, the thermodynamic equilibrium voltage must be higher than 1V [36, 49]. In general, low coulombic efficiency for the initial cycle is found to be one of the disadvantages and higher voltages versus Li/Li+ compared to carbon anodes except Cr_2O_3 and MnO put a decrease to the energy density and cell voltage [48].

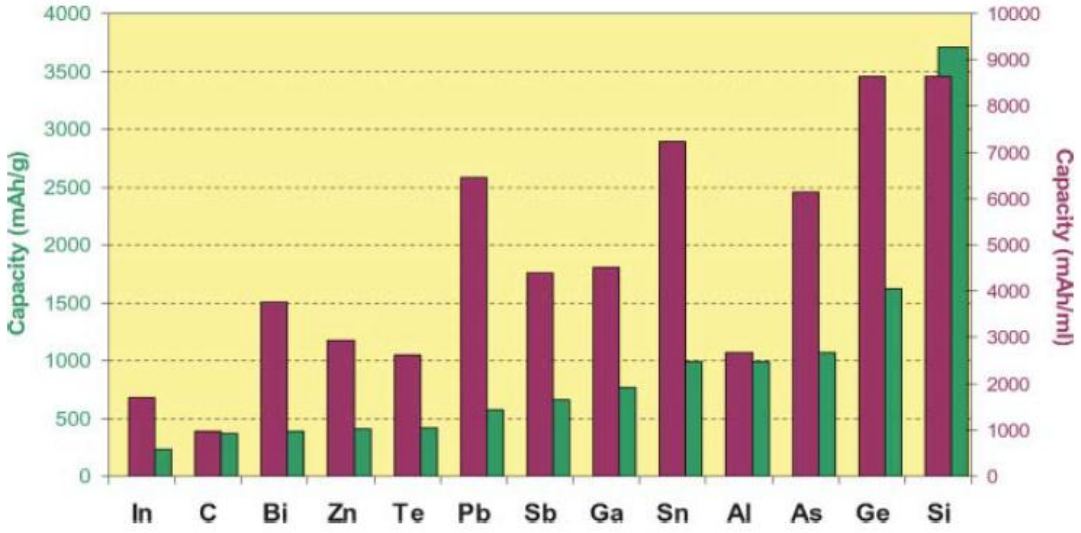

Figure 2.9 Gravimetric and volumetric capacities for selected alloying reactions. Capacities for graphite are given as references [51].

2.1.4.3 Electrolyte

In addition to the cathode and anode, electrolyte is another significant component in lithium-ion batteries. In a lithium-ion battery system, the electrolyte acts as a medium to transport lithium ions which participate in the charge/discharge process. Electrolyte is often composed of organic solvent due to the high voltage generated by the cell [50]. The common solvents in the electrolyte include ethylene carbonate (EC), dimethyl carbonate (DMC), and diethyl carbonate (DEC), with a lithium salt, such as $LiPF_6$, $LiBF_4$ and so on [50]. The ionic conductivity of a typical electrolyte is 10^{-2} S cm^{-1} at room temperature

and that will increase with increasing temperature [50]. With the development of lithium-ion batteries, many new forms of electrolyte were developed as it is shown in the Table 2.2.

Table 2.2 Behaviour of cation-conducting electrolyte materials [52].

Phenomenon/environment	Electrolyte behavior		
	Polymer	Liquid	Solid
Matrix	Flexible	Mobile	Fixed
Position of ion sites	Changes as chains flex	None	Fixed; accessibility affected by temperature
Solution	Yes	Yes	Not really
Solvation	By matrix: roll-on mechanism	Forms mobile solvated ions	No
Concentration of solute	Really high	Often low	Usually does not apply
Participation of charged ion clusters	Often yes	Usually no, except in molten salts	No
Contribution from migration of neutral species	Important	Usually unimportant	No
High cationic transference number	Usually no	Usually yes	Often unity for cation conductors

Utilization of solid electrolyte makes the cell design easier, as well as improves the safety, reliability and durability. Based on the materials used, there are two types of solid

electrolyte: inorganic ceramics and organic polymers [53]. The most obvious difference between these two kinds electrolyte is the elastic moduli, and ceramic has a higher elastic moduli as well as high temperature tolerance [53]. One of the most important properties to evaluate the electrolyte is the ionic conductivity. It was found that for ceramic electrolyte like $Li_2S - P_2S_5$, with increasing temperature, the ionic conductivity increases and the material with higher crystallinity always demonstrate higher ionic conductivity and lower activation energy [53-56]. In addition, the most common polymer used for making electrolyte is poly(ethylene oxide) (PEO) which is a good lithium-ion conductor. For different Li salts dissolved into PEO like lithium trifluoromethanesulfonate ($LiCF_3SO_3$) (LiTf) lithium bis(trifluoromethanesulfonimidate) ($Li(CF_3SO_2)_2N$) (LiTFSI) and so on, they have a pretty close range of ionic conductivity between each other [53].

Although selection of electrolyte depends on the particular battery design, the advantages of solid and polymer electrolyte are attracting more and more attention and develop rapidly.

2.1.4.4 Separator

Generally speaking, separator is a polymer membrane sandwiched between anode and cathode to prevent direct contact of two electrodes which will cause short circuit. Besides, material that is used for separator must be permeable for ionic flow. Although separators don't involve in the chemical reaction among anode, cathode and electrolyte, they play a key role in determining the performance of the lithium ion batteries. The rapid development of lithium ion battery industry and the appearance of novel lithium ion

batteries have witnessed the development of new separators [57].

In order to attain good performance and safety in a battery, there are some basic requirements for the separators like electronic insulator, mechanical and dimensional stability, sufficient physical strength, adequate thickness and so on [57]. Currently, the membranes used for commercial lithium-ion batteries are mainly made of microporous polyolefin which are thin (20-30 μm) and have porosity of 30-50% [57] [58]. As it is shown in the Table 2.3, polyethylene (PE) and polypropylene are the two dominant materials that are used to produce lithium-ion battery separators and wet and dry method are respectively utilized for these two different materials [57].

Table 2.3 Major manufacturers of lithium-ion battery separators along with their typical products [57].

manufacturer	structure	composition	process	trade name
Asahi Kasai	single layer	PE	wet	HiPore
Celgard LLC	single layer	PP,PE	dry	Celgard
	multilayer	PP/PE/PP	dry	Celgard
	PVDF coated	PVdF, PP, PE, PP/PE/PP	dry	Celgard
Entek Membranes	single layer	PE	wet	Teklon
Mitsui Chemical	single layer	PE	wet	
DSM	single layer	PE	wet	Solupur
Nitto Denko	single layer	PE	wet	
Tonen	single layer	PE	wet	Setela
Ube Industries	multilayer	PP/PE/PP	dry	U-Pore

For lithium-ion battery separators, the thickness must be limited to certain degree because increased thickness will lower the amount of active materials that can be placed in the battery [57]. In addition, the separator must be able to absorb and retain the liquid electrolyte, however, for currently used PE separators, because of its hydrophobic property, its compatibility with liquid electrolyte is not satisfactory [59]. Besides, the low

thermal stability of PE separators will cause safety problems like battery explosion in use [60]. As it is shown in the Table 2.4, the performance of the cell is closely related to the properties of the separators [57].

Table 2.4 General requirements for lithium-ion battery separator [57].

parameter	goal
thickness (μm)	<25
electrical resistance (MacMullin no.dimensionless)	<8
electrical resistance (ohms cm^2)	<2
gurley (s)	~25/mil
pore size (μm)	< 1
porosity (%)	~ 40
puncture strength (g/mil)	>300
mix penetration strength (kgf/mil)	>100
shrinkage (%)	<5% in both MD and TD
tensile strength (%)	<2% offset at 1000 psi
shutdown temp (℃)	~130
high-temp melt integrity (℃)	>150
wettability	complete wet out in typical battery electrolytes
chemical stability	stable in battery for long period of time
dimensional stability	separator should lay flat; be stable in electrolyte
skew (mm/m)	<0.2

Currently separators are produced by either dry or wet process [57]. In terms of these two methods, one or more orientation steps are needed to increase the porosity and the

tensile strength [57]. In the process of dry method, the polymer will be first melt into a polymer resin and then extrude it into a film [61]. The annealed film will be precisely stretched to form tightly ordered micropores [61]. After the initial extrusion, a nonporous structure is often formed with a high orientation, and then the stretching process actually formed the micropores [57, 61]. The dry method is very convenient and environmentally friendly because there is no need of solvent in the entire process [57]. On the other hand, the wet process, initially involves producing mixture of polyolefin resin with hydrocarbon liquid or some other low molecular weight substance and melting the mixture [57, 62]. The melt mixture is extruded into a membrane, and orientating the sheet either in the machine direction (MD) or biaxially before extracting the solvent with a volatile solvent [57, 62]. Ultrahigh-molecular-weight polyethylene (UHMWPE) can be used in this method to produce separators which have very good mechanical properties [57, 63]. Typical microporous structures of polyethylene and polypropylene separators are shown in Figure 2.9 [57].

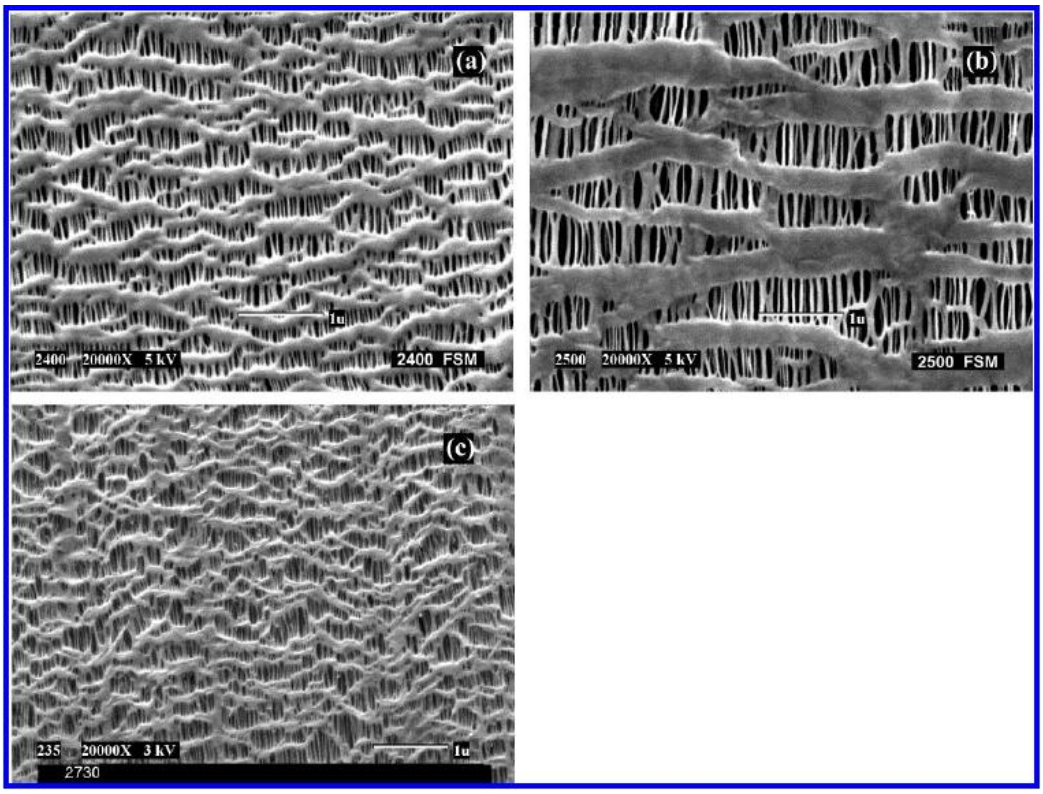

Figure 2.10 Scanning electron micrographs of Celgard separators used in lithium-ion batteries: (a) 2400 (PP), (b) 2500 (PP), and (c) 2730 (PE) [57].

With the rapidly increased demand for energy, more research efforts are being focused on separators to optimize their properties.

2.2 Electrospinning and Electrospun Nanofibers

2.2.1 Overview of Electrospinning

Because of the large surface area to volume ratio, nanofibers have a great potential to improve the properties of current materials and be applied in many novel applications [64]. Compared with traditional materials, nanofibers have many advantages in flexibility, surface functionality, mechanical properties and so on [65]. Due to the merits of the nanofibers, they have been used in many fields such as environmental and energy applications [66], tissue engineering applications [67]. For application in the

environmental and energy application, the nanofibers have found its strength in super-capacitors, fuel cells and battery separators [66]. Electrospinning, as one of the most efficient methods to produce the nanofibers directly from the polymer solutions, has attracted lots of attention in the last 10 years.

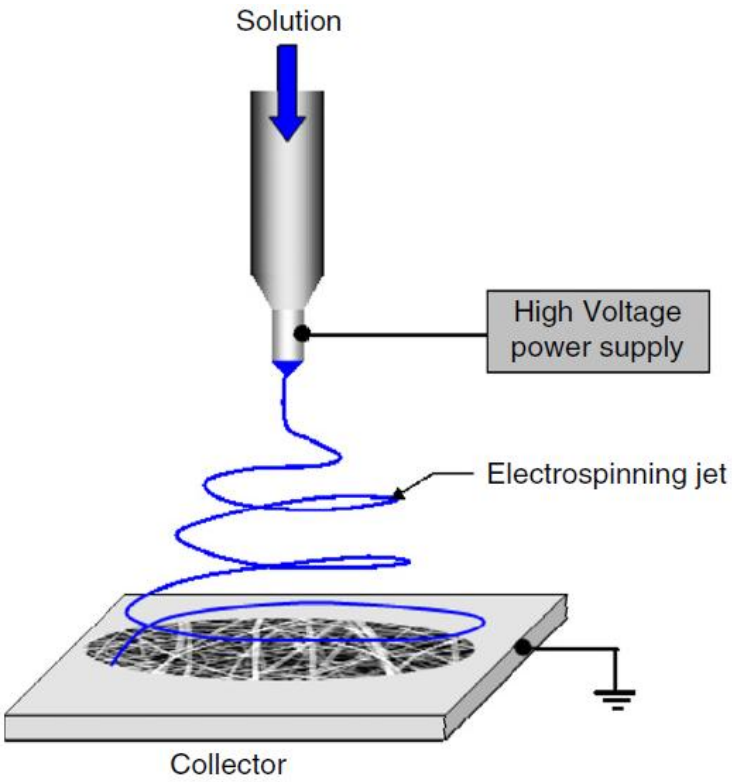

Figure 2. 11 A typical electrospinning set-up using a grounded static collector [64].

A typical electrospinning set-up consists of a syringe with a metallic needle, a metallic collector and a high voltage supplier as it is shown in the Figure 2.9. The applied high voltage is used to produce repulsive force on the polymer solution which can overcome the surface energy of the polymer solution and erupt the liquid electrospinning jet from the tip of the needle to form nanofibers on the collector.

2.2.2 Influencing parameters in electrospinning

Based on the different kinds of fibers, in order to control the morphology of the electrospun nanofibers, we can adjust the processing parameters to achieve adequate properties through studying the similar and different properties of these fibers.

In general, parameters that will have effects on the morphology of the nanofibers include viscosity of the solution, polymer molecular weight, flow rate, dielectric constant, voltage, the distance between needle tip and the collector and so on.

In general, variation in the viscosity of polymer solutions can bring great change on the morphology of the nanofibers [68]. There is a range for the polymer solutions within which the polymer can be electrospun, for example, in Fig 1, when the poly(D,L-lactic acid) (PDLA) solution is 20 wt%, continuous nanofibre cannot be collected, on the other hand, when the polymer solution concentration is increased to 40 wt%, the electrospinning process is also difficult to process due to the high viscosity and the solution droplet will be dried out before it is jetted out [68]. That is because at low concentration, the surface tension is the dominant parameter for the fiber formation process, below some specific concentration beads will be formed instead of fibers [68].

In addition to the exterior influencing parameters, the electrospun nanofibers will also react to polymer and solvent properties we use. For example, Molecular weight is almost the most direct influencing parameter for the polymer properties. The variation of the molecular weight will bring significant effect on the rheological properties, electrical

properties, dielectric strength, and surface tension in the polymer solution [75]. Based on Flory's theory [76], the higher molecular weight will lead to a higher viscosity polymer solution. When processing the electrospinning, compared with lower molecular weight polymer, higher molecular weight polymer solution often need higher flow rate to eliminate the junctions between fibers. Other parameters like tacticity and entanglement of polymers also influence the electrospinnability morphology significantly [77, 78].

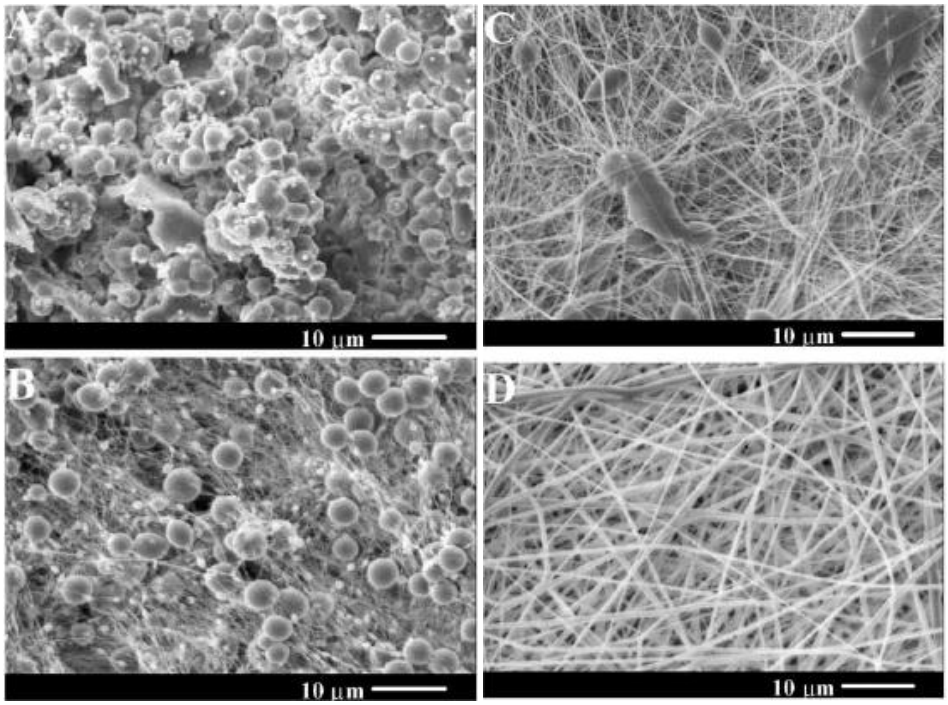

Figure 2.12 Concentration effect on microstructures of electrospun poly(D,L-lactic acid) nanofibers at voltage of 20 kV, feeding rate of 20 ml/min, and concentration of (A) 20 wt%; (B) 25 wt%; (C) 30 wt% and (D) 35 wt%. [68].

Applied voltage is another decisive factor that can change the fiber morphology dramatically. It has been confirmed that changing the voltage can alter the shape of the initiating polymer solution droplet at the exit tip [69]. For the electrospun mats,

increasing the voltage will cause a slight increase in the diameter of the nanofibers, however, a lower fiber diameter distribution can be achieved when the applied voltage is relatively low [70]. On the other hand, higher voltage will bring another problem which is that higher voltage will produce more neutralizing ions at the tip of needle and then more bead defects will emerge on the electrospun mats as shown in the Fig 2.12 [71].

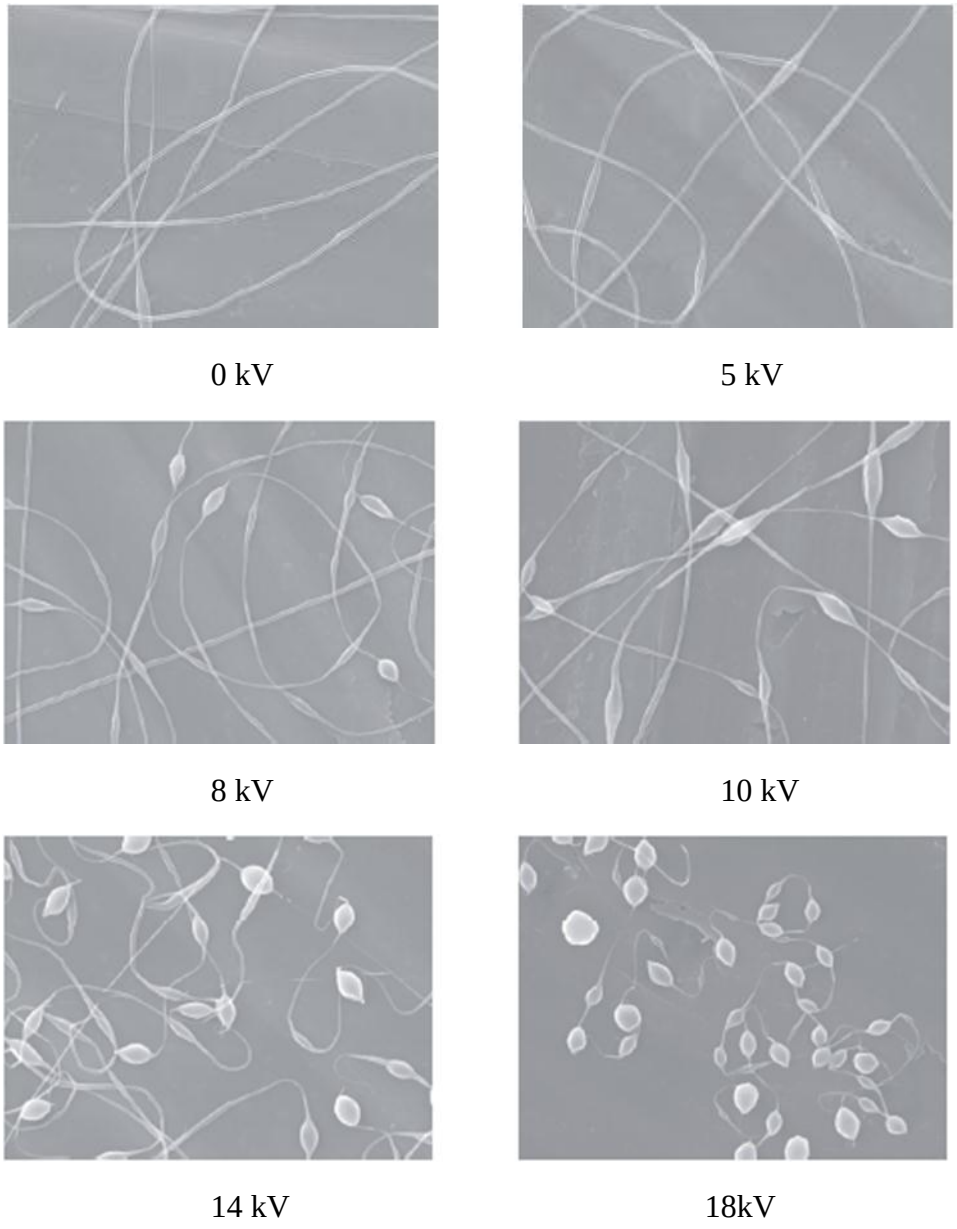

Figure 2.13 Effect of voltage on the morphology of nanofibers jet through the air. Electrospun from 3.85 wt% poly(ethylene oxide) in water. Electric field is 0.4 kV/cm. The horizontal edge of each of the figures is 20 microns long [71].

In terms of the distance between needle tip and the collector, there is a minimum distance between tip and collector for the fiber formation because sufficient time should be provided to allow the fiber to dry before it reaches the collector [71]. However, some research results demonstrate that tip-collector distance has limited effect on the

morphology of the electrospun mats.

There are also studies that have shown the effect of the solvent on the morphology of the electrospun fibers. For example, a research processed the electrospinning of polystyrene in 18 different solvents, however, only the solvents with higher values of dipole moment showed better morphology of nanofiber mats [67].

There are some ambient parameters that will also have an obvious effect on the morphology of electrospun nanofibers. Humidity of the atmosphere has been shown to directly influence the morphology of the electrospun fibers. Different polymers have been electrospun under different humidity conditions to show the effect of humidity on the surface features of the fibers [74]. For example, as Fig 2.13 shows, under different humidity atmosphere which is the only changing parameter in the experiment, with increased humidity, some uniform, circular pores are distributed on the surface of the polystyrene (PS) fibers at first [74]. When the humidity keep increasing to about 50-59 %, the shape of the pores become nonuniform and the pore density is significantly enhanced [74].

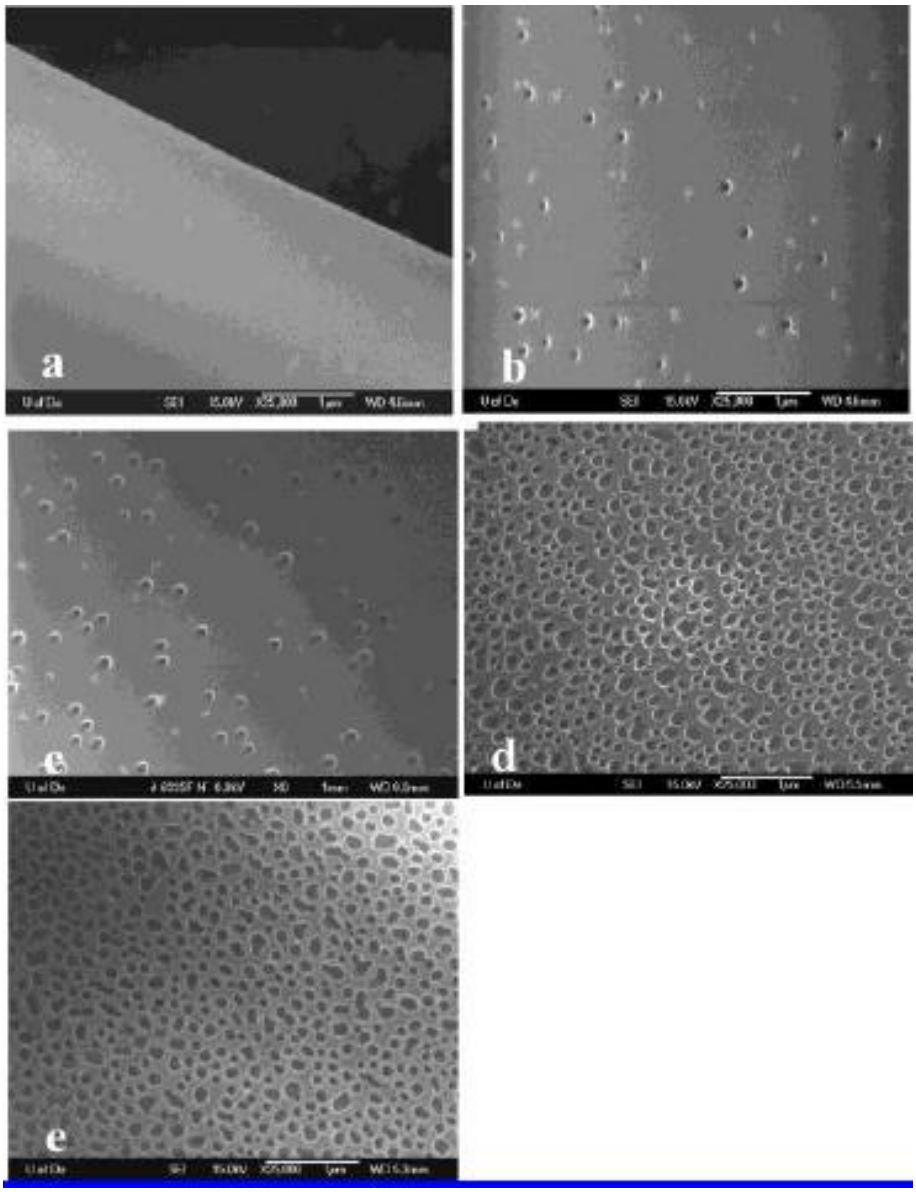

Figure 2.14 FESEM micrographs of 190 000 g/mol PS/tetrahydrofuran fibers electrospun under varying humidity: (a) <25%, (b) 31-38%, (c) 40-45%, (d) 50-59%, (e) 60-72% [74].

Chapter 3 Research Objectives

3.1 Fabrication of Polyvinylidene Fluoride (PVdF) Nanofiber Membranes through Electrospinning for Use as Separators in Lithium-ion Batteries.

Separator as one of the most important components for lithium-ion batteries is closely related to the battery safety and performance. Common materials that are currently utilized to produce lithium-ion separators are polypropylene (PP) and polyethylene (PE) since they have excellent mechanical strength and chemical stability. However, the poor wettability, and relatively low melting and glass transition temperature of polyolefin materials hinder the full realization of the excellent performance of lithium-ion batteries.

Electrospinning, a simple and efficient way to produce nanofibers, has been widely applied for many different polymers, ceramics, and other materials. Through electrospinning, nanofiber-based nonwoven membranes made of different materials can be obtained. Besides, by controlling the electrospinning parameters like applied voltage, eruption rate of polymer solution and so on, different nanofiber morphologies can be developed. Compared with larger-sized fibers, nanofiber membranes have significantly improve wettability due to their large surface area which is desirable for the application of lithium-ion battery separators.

In this work, PVDF was used as the raw material to produce electrospun nanofiber membranes. The electrospun PVDF nanofiber membranes have relatively large surface area, which leads to good wettability property. In addition, hot-press treatment was processed to improve the mechanical properties of the electrospun PVDF nanofiber

membranes.

3.2 Fabrication of Nanofiber-coated Nonwoven Polypropylene Composite through Electrospinning and Hot-pressing Treatment for Use as Separators in Lithium-ion Batteries.

In addition to wettability, mechanical property is also essential in evaluating the performance of lithium-ion battery separators because they must be able to withstand the tension developed by the winding operation during battery assembly.

In order to take full advantage of the good mechanical properties of polypropylene and high porosity of nonwoven, we select the polypropylene nonwoven fabric as the base material and electrospun PVDF as the coating material to fabricate battery separators. The mechanically-strong PP nonwoven fabric has large porosity which is beneficial for the absorption of liquid electrolyte. On the other hand, the electrospun PVDF coating can improve the wettability and thermal properties of the resultant separator.

In this work, after the direct electrospinning of PVDF nanofibers on both sides of the PP nonwoven fabric, a hot-pressed process was applied on the composite to increase the adhesion of the electrospinning coating on the nonwoven substrate.

Chapter 4 Electrospun PVDF Nanofiber Membrane for Lithium-ion Battery Separators

Abstract

Polyvinylidene fluoride (PVDF) nanofiber membranes were prepared through electrospinning under three different applied voltages and followed by hot pressing treatment. The membrane produced at 20kV applied voltage shows relatively narrow fiber distribution, however the membranes with 15kV applied voltage exhibit more uniform and stable structure. Electrolyte uptake and ionic conductivity tests were processed by soaking the membranes into a liquid electrolyte consisting of 1 M lithium hexafluorophosphate ($LiPF_6$) dissolved in 1:1:1 (by volume) ethylene carbonate/dimethylcarbonate/ethylmethyl carbonate. It was found that the hot-press process slightly decreased the electrolyte uptake capacities and ionic conductivities of electrospun membranes by decreasing the membrane porosity. However, the hot-press increased the modulus, tensile strength, and strain at break. It can improve the tensile properties significantly due to the elimination of internal stress generated during electrospinning and the improvement of the crystalline perfection of PVDF in the membranes. The electrochemical stability window test exhibited that the influence of applied voltage and hot-press process on the electrochemical properties are relatively small. In addition, the coin-type $Li/LiFePO_4$ cells using hot-pressed PVDF and Celgard membranes as separators showed good cycling stability at room temperature. The results indicate that hot-pressed electrospun PVDF membranes are promising separator candidate

for lithium-ion batteries.

4.1 Introduction

High-performance and rechargeable lithium-ion batteries have attracted lots of attention due to their excellent energy capacity, power densities and long cycle life [79, 80]. Separator, which is sandwiched between the cathode and the anode to physically separate the two electrodes in prevent of short circuit, is important to attain good performance and safety for lithium-ion batteries [57].

Currently, the most commonly used materials to produce lithium-ion battery separators are polypropylene (PP) and polyethylene (PE) due to their excellent mechanical properties, chemical stability [57, 58]. However, considering the disadvantages of polyolefin separators like low wettability, and poor thermal stability [60], new separators are urgently needed to help realize the high performance potential of lithium-ion batteries.

Electrospinning as an efficient method to produce nanofibers has attracted lots of attention and many researchers have tried to prepare porous nanofiber membranes for use as lithium-ion battery separators like polyamide [79], PAN [84] [85], poly(methyl methacryate) (PMMA) [86]. Electrospun nanofiber separators made from these materials have rapid and high electrolyte uptakes. In general, fast electrolyte uptake makes the battery assembly process more rapid and the ability to retain the liquid electrolyte can give a longer life time for the lithium-ion battery [87].

In this chapter, the traditional electrospinning method was employed to produce PVDF nanofiber membranes for use as the lithium-ion battery separators. PVDF was selected as the polymer to produce separators because it has good chemical stability, good

mechanical properties, high glass transition and melting temperature, and excellent adhesion properties. However, due to the small diameter of nanofibers, the mechanical properties of nanofiber membrane are poor. Therefore, the hot-press process was used to improve the mechanical properties of these PVDF nanofiber membranes. Based on the fact that electrospinning parameters will impact the morphology of the nanofiber membranes, different applied voltages were used to investigate the effect of different nanofiber morphology on the separator performance.

4.2 Experimental

4.2.1 Materials

PVDF (O-Fluorine Chemical Technology, ShangHai, #904) with a molecular weight 600,000 g/mol, was used as the polymer to produce lithium-ion battery separator. The solvent used was a mixture of N,N-dimethylformamide (DMF) (Sigma-Aldrich, ≥99.8%) and acetone (Sigma-Aldrich, ≥99.8%) with a ratio of 9:1 by volume. The liquid electrolyte consisted of 1 M lithium hexafluorophosphate ($LiPF_6$) dissolved in 1:1:1 (by volume) ethylene carbonate/dimethylcarbonate/ethylmethyl carbonate. The electrodes sued in cell performance were lithium metal electrodes (Sigma-Aldrich, 99.9%, 0.38mm thickness) and $LiFePO_4$ electrodes, consisting of active material $LiFePO_4$ (80wt.%, Hydro-Qubec), acetylene black (10 wt.%, Fisher Scientific) and polyvinylidene fluoride binder (10 wt.%, Aldrich).

4.2.2 Preparation of nanofiber separators

The electrospinning solution (10 wt% PVDF in mixture of DMF and Acetone, 9:1) was mechanically stirred at room temperature for 24 h before electrospinning. Nanofiber membranes were prepared by the electrospinning method with 3 different applied voltages. The polymer solution was pumped to the top of the needle, and a Taylor cone was formed by applying three different high voltages (10kV, 15kV and 20kV). Under each voltage, when the repulsive force within the charged solution was larger than its surface tension, a jet would erupt from the tip [64]. The solvent evaporateed in this process and dry polymer fibers are deposited on the collector.

During electrospinning, the distance between syringe needle and collector was 15cm and the flow rate of polymer solution was 1.0 ml/h.

After electrospinning process, all the as-prepared nanofiber membranes were carefully washed using ethanol to remove the impurities. After this process, the membranes were kept in the vacuum oven with a temperature 40 ℃ for 3h to remove the solvent residual.

The hot-press process was conducted on nanofiber membranes electrospun at 15kV applied voltage. The hot-press temperature used in the hot-press process was 100 ℃, the pressure of 500 psi and the hot-process time was 10 min. The thickness of all prepared PVDF nanofiber membranes was in the range of 40 μm to 63 μm.

4.2.3 Structure characterization and property measurements

The morphology of PVDF nanofiber membranes was investigated using a scanning

electron microscopy (JEOL 6400F Field emission SEM) with an acceleration voltage of 10 kV. In order to reduce charging, the PVDF membranes were coated with Au by a K-550X sputter coater prior to the SEM observation. The nanofiber diameter data was obtained by measuring fifty fibers randomly selected in SEM images using Revolution v1.6.0 software.

Electrolyte uptake test was conducted by soaking pre-weighted separator membranes into a liquid electrolyte for a specific time at room temperature in the glove box filled with protecting argon gas. The electrolyte used consists of 1 M lithium hexafluorophosphate ($LiPF_6$) dissolved in 1:1:1 (by volume) ethylene carbonate/dimethylcarbonate/ethylmethyl carbonate. The soaked membranes were weighted again after removing the excess electrolyte solution adhering to the membrane surfaces by gently wiping with filter paper. The electrolyte uptakes were calculated by:

$$\textit{Electrolyte Uptake}\ (\%) = (W_f - W_0)/W_0 \times 100 \qquad (4.1)$$

where W_f and W_0 are the weights of the electrolyte-soaked membranes and dry membranes, respectively.

The mechanical properties of PVDF nanofiber membranes were measured using an Instron tensile tester. Prior to the tensile test, the membranes were cut into 1cm ×5cm size and the thickness of the samples were measured and recorded. In the process of the tensile test, the upper clip goes up at a constant rate until the sample breaks. Prior to the tensile test, the membranes were cut into 1cm × 5cm in size, and the thickness of the membranes were measured and recorded. During the tensile test, the upper clip moved up at a

constant rate until the membrane broke.

The ionic conductivities of the electrolyte-soaked PVDF nanofiber membranes were measured by electrochemical impedance spectroscopy (EIS) using Reference 600 Potentiostat/Galvanostat/ZRA (GAMRY). Before the measurement, the electrolyte-soaked membranes were sandwiched between two symmetrical stainless-steel plate electrodes and sealed in an argon-filled glove box. The measurement was performed with the amplitude of 10mV over a frequency range of 1000 kHz to 1Hz at a temperature range between 25 ℃ and 85 ℃. The intercept on the real-axis of the Nyquist plot gave the resistance R_b of the liquid electrolyte-soaked PVDF membranes. The ionic conductivity (σ) was calculated by:

$$\sigma = d / (R_b \times A) \tag{4.2}$$

where d is the membrane thickness, R_b the bulk resistance of liquid electrolyte-soaked membrane, and A is the cross-sectional area of the membrane.

The electrochemical stability windows of liquid electrolyte-soaked PVDF membranes sandwiched between stainless-steel and lithium counter electrodes were performed by linear sweep voltammetry using the Reference 600 Potentiostat/Galvanostat/ZRA (GAMRY) under the scan rate of $10mVs^{-1}$ and the potential range from 2.5V to 6V at room temperature.

The electrochemical performance of liquid electrolyte-soaked PVDF nanofiber membranes was evaluated in Li/$LiFePO_4$ cells assembled in the glove box filled with argon gas. Charge and discharge were conducted using an Arbin automatic battery tester

in the potential window of 2.5 – 4.2 V at 0.2 C.

4.3 Results and Discussion

4.3.1 SEM

The SEM images of electrospun PVDF membranes prepared under three different applied voltages were shown in the Figure 4.1. It is seen that when the applied voltage is 10 kV, polymer beads are formed. When the applied voltage increases to 15kV, the beads disappear. As the applied voltage increases to 20 kV, fibers become thinner but exhibit rougher surface.

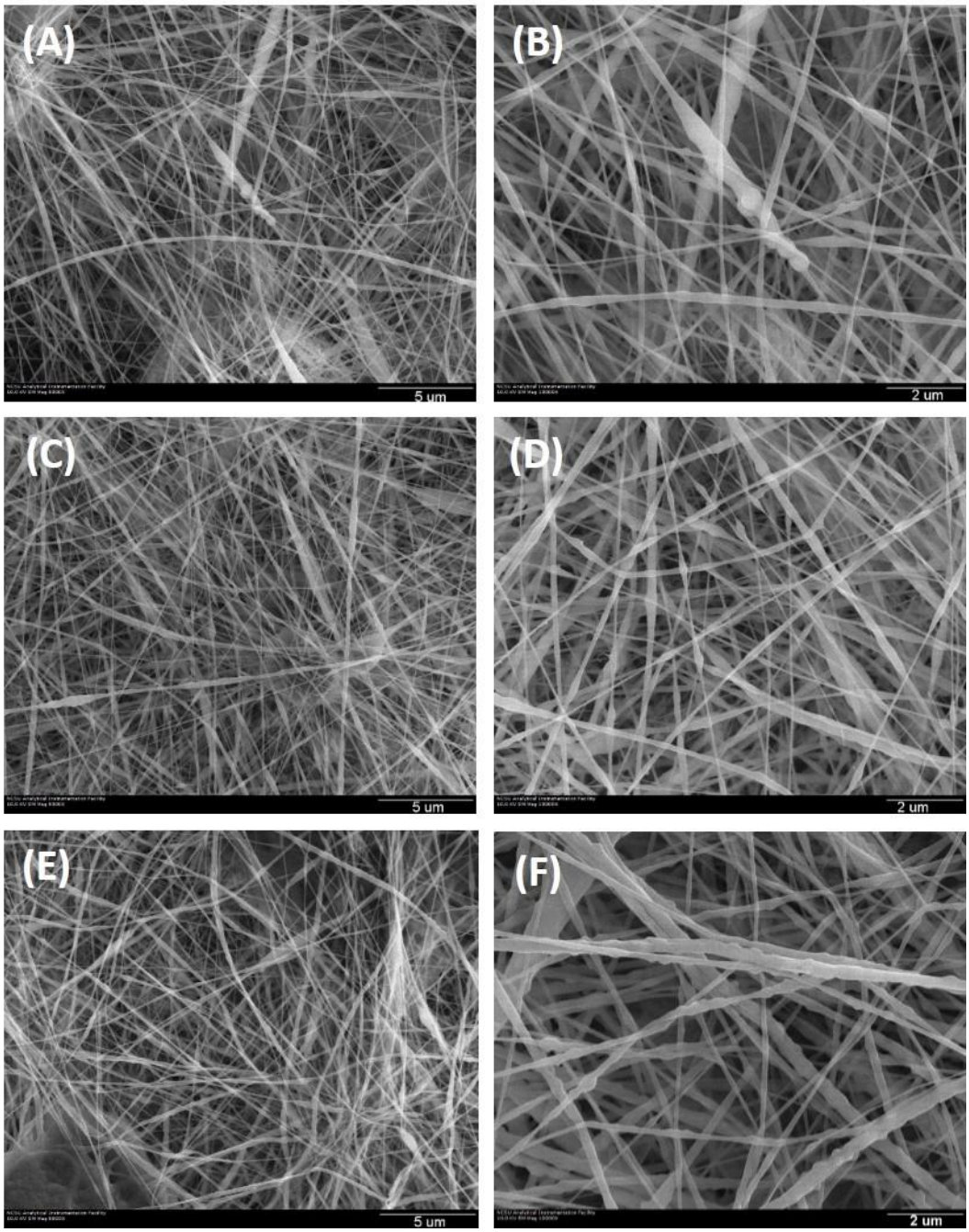

Figure 4.1 SEM images of electrospun PVDF membranes prepared with different voltages: (A, B) 10kV, (C, D) 15kV, and (E, F) 20kV.

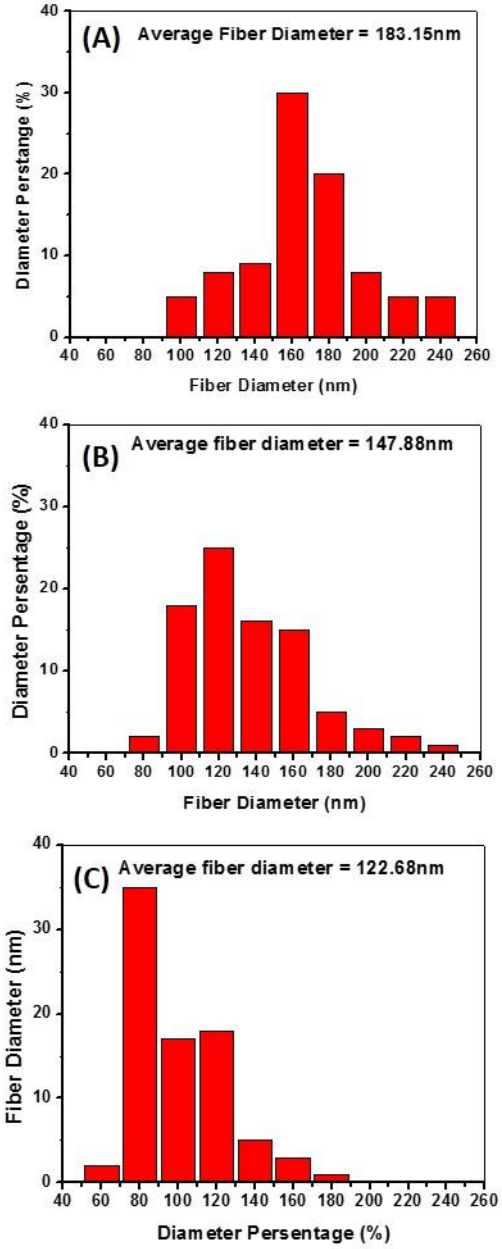

Figure 4.2 Diameter distribution of electrospun PVDF fibers prepared with different voltages: (A) 10kV, (B) 15kV, and (C) 20kV.

Figure 4.2 shows the fiber diameter distributions of electrospun PVDF membrane under different applied voltage. With increase in the applied voltage, the average fiber diameter decreases as expected. When the applied voltage becomes 20kV, the fiber

diameter has a relatively narrow range.

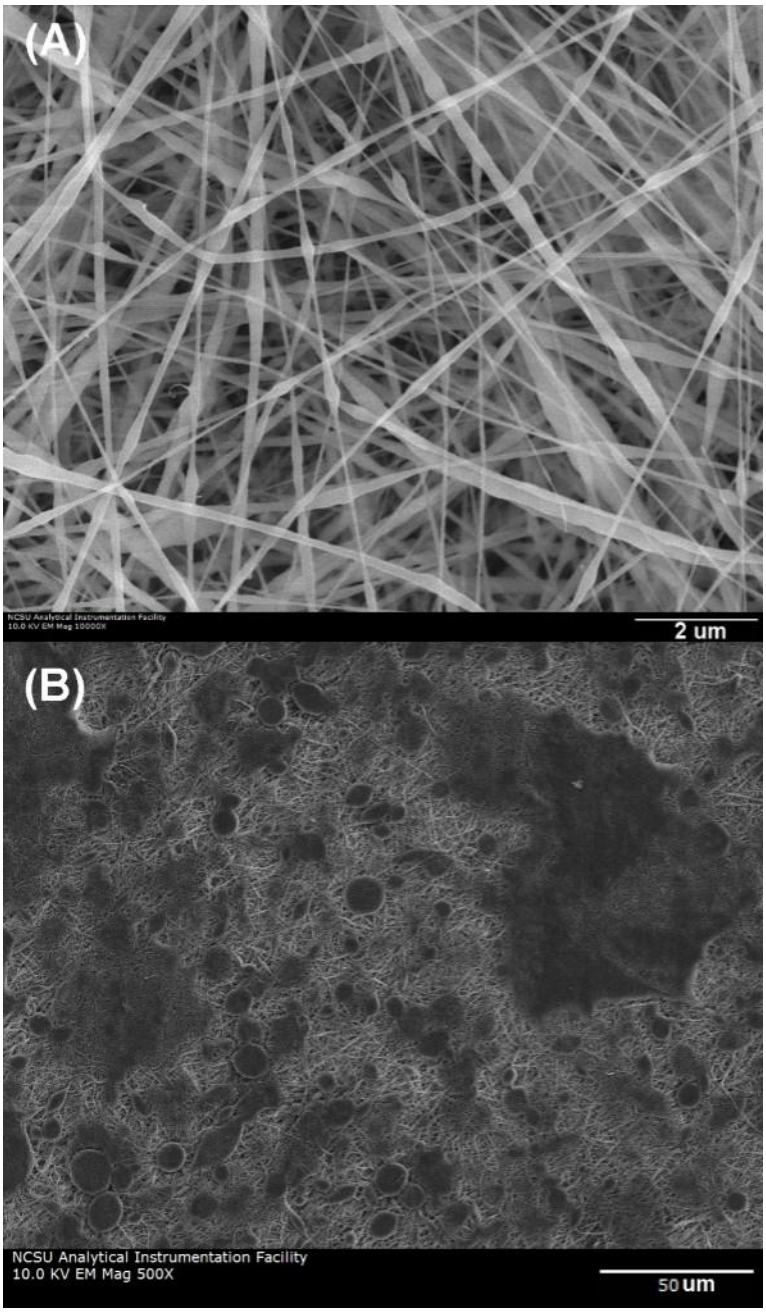

Figure 4.3 SEM images of electrospun PVDF membranes (A) before, and (B) after hot-press.

Figure 4.3 compares the morphologies of electrospun nanofiber membranes before

and after hot-press. It is seen that in the hot-pressed membrane, there are some molten fiber aggregates caused by the hot-press which could decrease the membrane porosity.

4.3.2 Tensile properties

Tensile properties of separators are important during battery assemble process since the separators have to be strong enough to withstand during winding force during cell winding and assembly [57].

Table 4.1 Average tensile strength, modulus, and strain-at-break of un-pressed and hot-pressed electrospun PVDF membranes.

	Strength (MPa)	Modulus (MPa)	Strain-at-break (mm/mm)
Un-pressed	2.7	94.3	0.06
Hot-pressed	4.1	203.1	0.07

Table 4.1 shows the strength, modulus, and strain-at-break of un-pressed and hot-pressed PVDF nanofiber membranes. The PVDF nanofiber membranes were electrospun at 15 kV. As shown in Table 4.1, after hot press, the strength increases from 2.7 MPa to 4.1 MPa and the modulus increases from 94.3MPa to 263.4 MPa. However, the strain-at-break does not change apparently. The increase in strength and modulus should be caused by the improvement of the bonding between nanofibers, the elimination of internal stress generated during electrospinning, and the perfection of crystals of PVDF

in the membranes [112].

4.3.3 Electrolyte Uptake

Electrolyte uptake is an important property parameter that indicates the ability of a membrane to absorb and maintain liquid electrolyte. The requirement for a good lithium-ion battery separator is that the separator can be completely and quickly wetted out in the typical liquid electrolyte [57]. A membrane with lower wettability limits the performance of the battery by increasing the cell resistance [57].

Figure 4.4 shows the electrolyte uptakes as a function of time between electrospun PVDF membranes under different applied voltages. For comparison, the electrolyte updates of a commercially-available Celgard 2400 membrane are also shown. The absorption rates of all four membrane are quick and the electrolyte uptakes are saturated in the first 100 seconds for each membrane. As shown in Figure 4.4, compared with Celgard membranes, the electrospun PVDF membranes have higher electrolyte uptake. The improvement in the electrolyte uptake is mainly due to the increased porosity and capillary effect of the electrospun nanofibers [111]. Besides, the polar groups in the chemical structure of the PVDF also contribute to the higher electrolyte uptakes of electrospun PVDF membranes. From Figure 4.4, it is also seen that the electrolyte uptake of electrospun PCVD membranes increases with increase in applied voltage. In general, the electrolyte uptakes of nanofiber membranes are closely related to the surface area of the fibers, and membranes with smaller diameter fibers have relatively larger surface areas [111]. As shown in Figure 4.5, when the applied voltage used for electrospinning

process is 20kV, the resultant membrane has the largest electrolyte uptake, which corresponds to the fact that larger applied voltage leads to thinner fibers (Table 2.1).

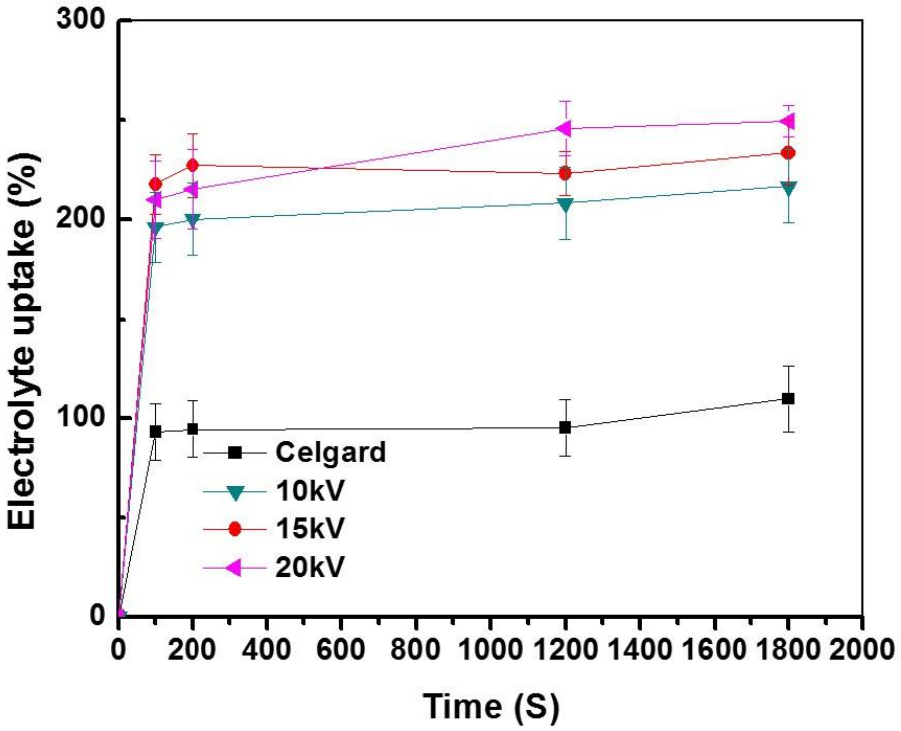

Figure 4.4 Electrolyte uptakes as a function of time for Celgard membrane and PVDF membranes prepared under different applied voltages: 10kV, 15kV and 20kV.

Figure 4.5 compares the electrolyte uptakes of un-pressed and hot-pressed PVDF nanofiber membranes. It is seen that the hot-press process reduced the electrolyte uptake capacity due to the partial shut-off of the pores of electrospun nanofibers occurred at the high hot-press temperature. However, even after hot press, the electrolyte update of PVDF membrane is still higher than that of the Celgard membrane.

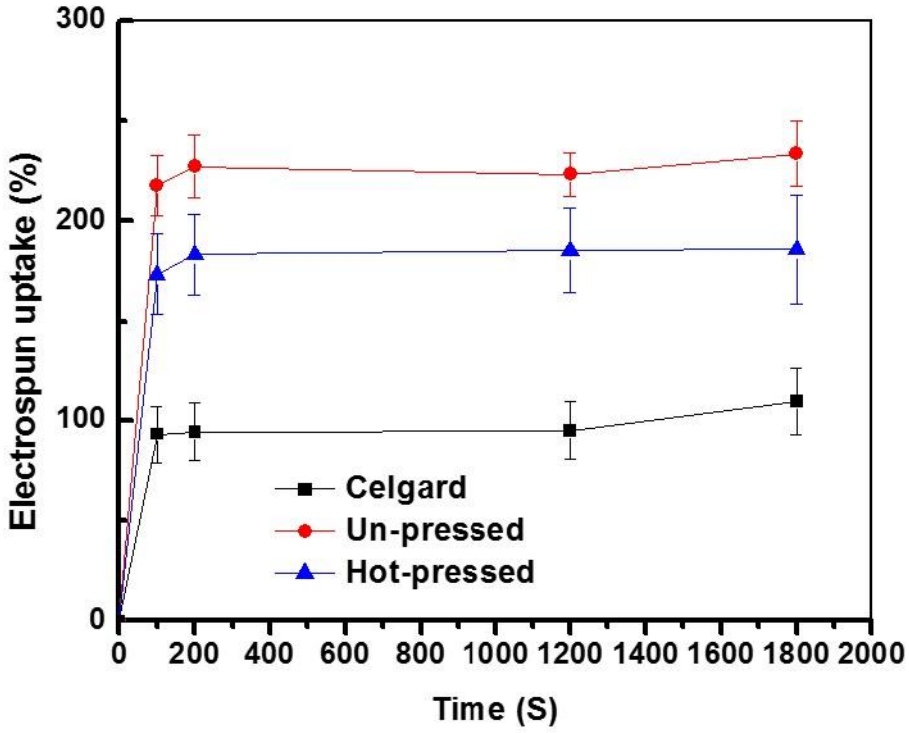

Figure 4.5 Electrolyte uptakes as a function of time for Celgard membrane and un-pressed and hot-pressed electrospun PVDF membranes.

4.3.4 Ionic Conductivity

The ionic conductivity of liquid electrolyte-soaked separator membrane is a function of the conductivity of the liquid electrolyte, and the porosity, tortuosity, and the wettability of the liquid electrolyte-soaked membrane [114]. The ionic conductivities results of liquid electrolyte-soaked PVDF membranes under different applied voltages are shown in the Figure 4.6. For comparison, the conductivities of liquid electrolyte-soaked Celgard membrane is also shown. For these four membranes, the ionic conductivities increase as the temperature increases due to the enhanced mobility of ions at higher temperatures

[113].

At all temperatures, the ionic conductivities of electrospun PVDF membranes are higher than the Celgard membrane, which is the result of their higher electrolyte uptake capacities. From Figure 4.6, it is also seen that the membranes show similar ionic conductivities when the voltage used for electrospinning changes. That is because the different applied voltages only have limited effect on the morphology of the electrospun PVDF membranes.

Figure 4.7 shows the effect of hot press process on the ionic conductivities of liquid electrolyte-soaked PVDF membranes. The hot press process decreases the ionic conductivities of liquid electrolyte-soaked PVDF membranes due to the reduced electrolyte uptake. However, at all temperatures, the ionic conductivities of hot-pressed membranes are still higher than those of liquid electrolyte-soaked Celgard membrane.

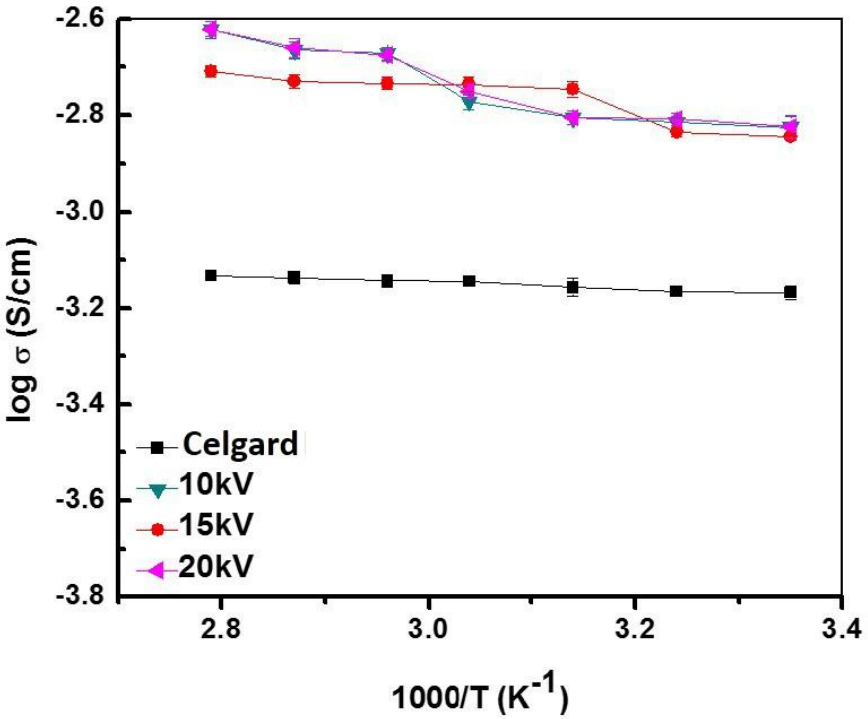

Figure 4.6 Ionic conductivities of liquid electrolyte-soaked Celgard membrane and electrospun PVDF membrane under different voltages: 10kV, 15kV, 20kV and as a function of temperature.

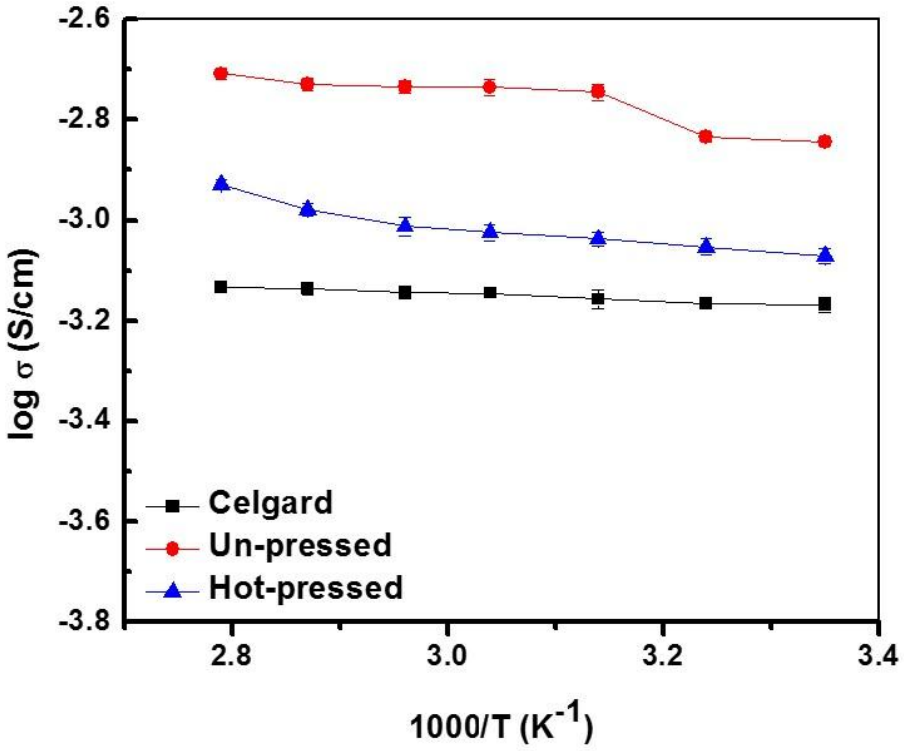

Figure 4.7 Ionic conductivities of Celgard membrane, and un-pressed and hot-pressed electrospun PVDF membranes as a function of temperature.

4.3.5 Electrochemical Stability Window

Kinetic electrochemical stability window is another important parameter in evaluating the performance of lithium-ion battery separators. The onset of a steady increase in the voltage under specific current density corresponds to the anodic stability limit of the liquid electrolyte-soaked membrane [115-117]. In general, the electrochemical stability window of liquid electrolyte-soaked separator membrane is mainly determined by the stability of the liquid electrolyte. However, the use of electrochemically-unstable separator could reduce the stability window of liquid electrolyte-soaked separator

membrane.

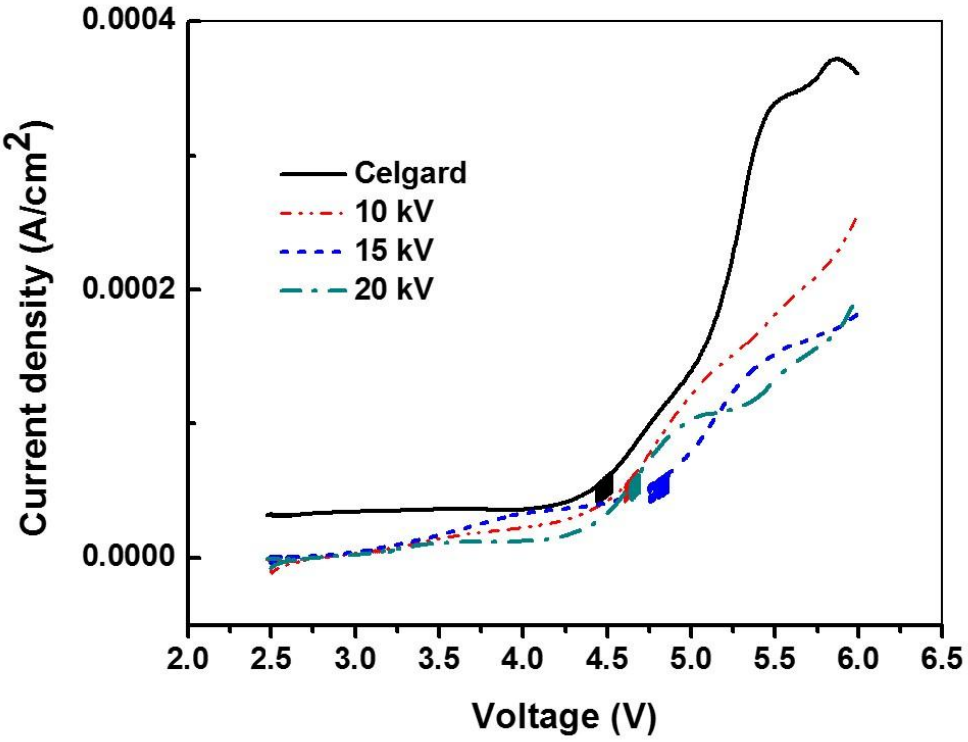

Figure 4.8 Electrochemical stability windows of Celgard and electrospun PVDF membranes with different applied voltages: 10kV, 15kV, 20kV.

Figure 4.8 shows the electrochemical stability windows of liquid electrolyte-soaked electrospun PVDF membranes. For comparison, the electrochemical stability window of liquid electrolyte-soaked Celgard membrane is also shown. It is seen that all four liquid electrolyte-soaked membranes are electrochemical stable when the voltage is below 4.5 V. The effect of hot-press on the electrochemical stability window is shown in Figure 4.9. It is seen that hot-press reduces the electrochemical stability window of liquid electrolyte-soaked electrospun PVDF membranes slightly, but the resultant stability

window is still comparable to that of liquid electrolyte-soaked Celgard membrane. The high electrochemical stability of liquid electrolyte-soaked PVDF membranes indicates that they can be used for most practical cathode materials.

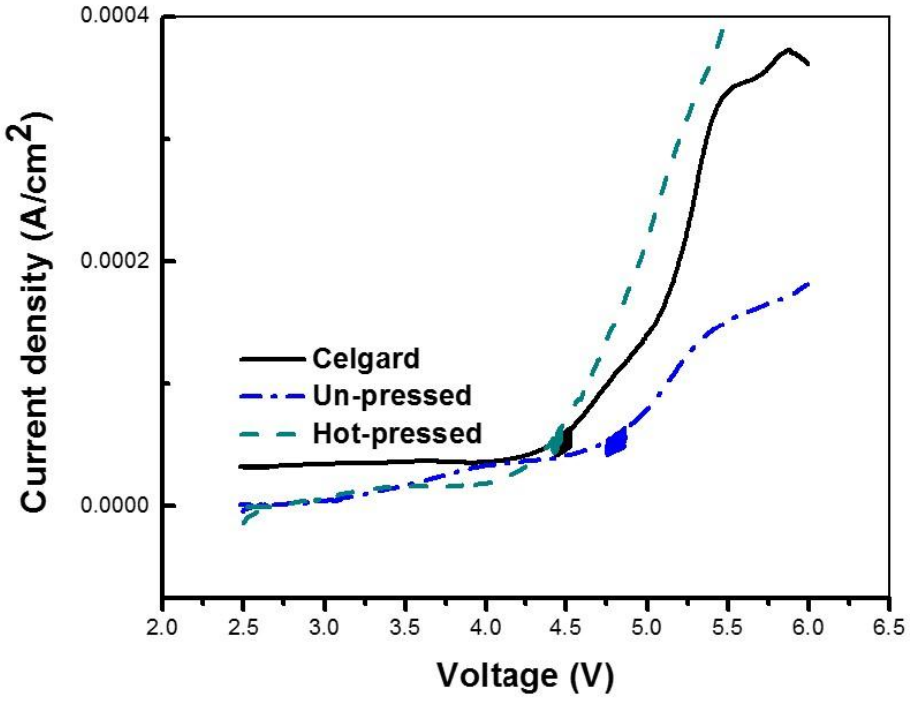

Figure 4.9 Electrochemical stability windows of Celgard, and un-pressed and hot-pressed electrospun PVDF membranes.

4.3.6 Battery Performance

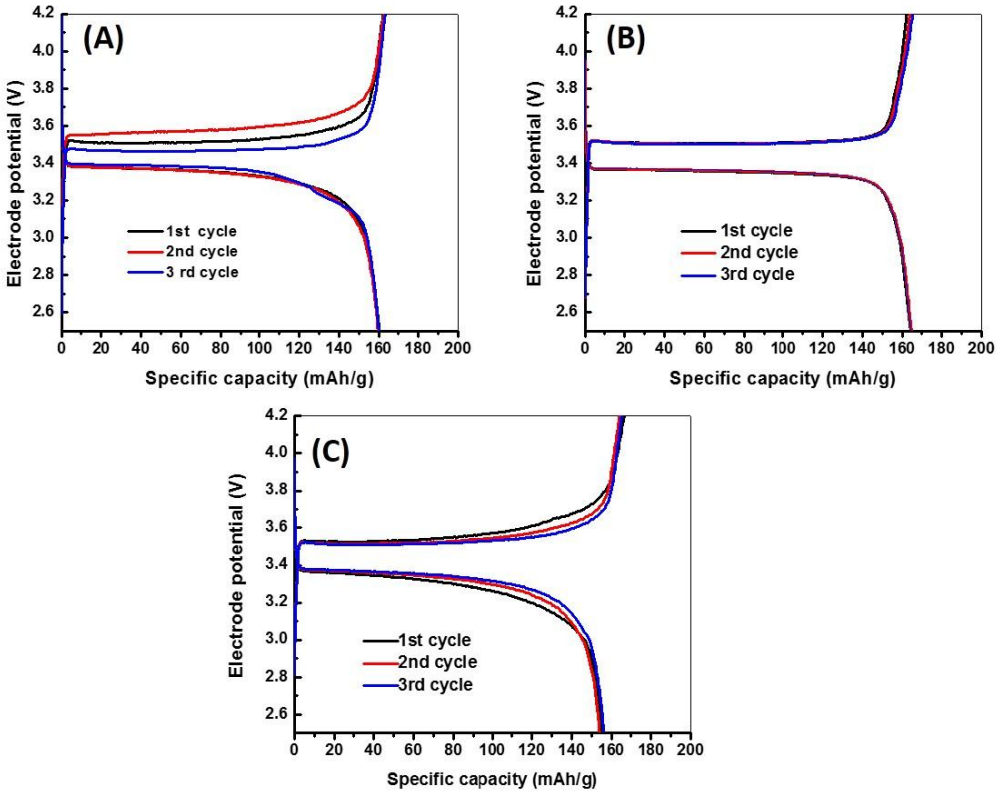

Figure 4.10 Charge-discharge curves of Li/$LiFePO_4$ cells containing: (A) Celgard, (B) un-pressed electrospun PVDF, (C) hot-pressed electrospun PVDF membranes.

Figure 4.10 shows the charge-discharge curves of the first 3 cycles of Li/$LiFePO_4$ cells containing Celgard, and un-pressed and hot-pressed PVDF membranes as the separators. The initial capacities of cells are 161, 163, and 158 mAh/g, respectively. Considering the theoretical capacity of $LiFePO_4$ (170 mAh/g), the charge-discharge performance of these cells are satisfactory.

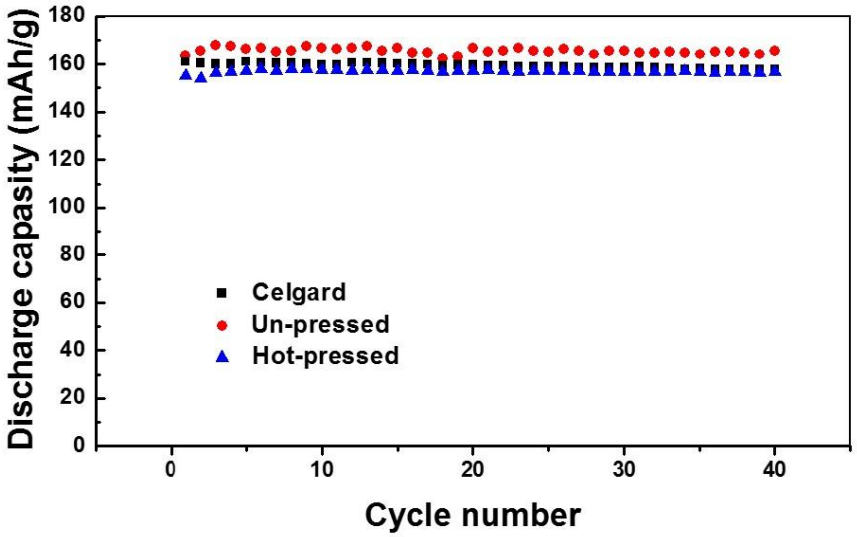

Figure 4.11 Cycle performance of Li/LiFePO$_4$ cells with Celgard membrane, un-pressed electrospun PVDF, membrane and hot-pressed electrospun PVDF membranes.

The cycling performance are shown in the Figure 4.11. Li/LiFePO4 cells containing Celgard, and un-pressed and hot-pressed PVDF membranes have discharge capacity of 157, 165, and 156 mAh/g respectively at the 40th cycle. For all three cells, the capacities remain stable during cycling, and show good capacity retention of almost 100% during the cycles. The results indicate that electrospun PVDF membranes have great potential to be used as lithium-ion battery separators and the hot-press process can improve the mechanical properties without sacrificing the electrochemical performance.

4.4 Conclusion

Electrospun PVDF nanofiber membranes were prepared under different voltages. The modulus, tensile strength, and strain-at-break were improved after the hot-press treatment. However, the electrolyte uptake capacity and ionic conductivity decrease slightly after the

hot-press due to the morphology change. The good cycling performance demonstrates that the hot-press does not have negative effect on the cell performance and the electrospun PVDF membranes are promising separator candidate for lithium-ion batteries.

Chapter 5 Electrospun PVDF-Coated Nonwoven Polypropylene for Lithium-ion Battery Separator

Abstract

Polyvinylidene fluoride (PVDF)-coated polypropylene (PP) nonwoven composite membranes were prepared by electrospinning. Hot-press treatment was used to enhance the adhesion between the electrospun PVDF coating layer and PP nonwoven substrate. In the tensile test, the electrospun PVDF-coated membrane exhibited high modulus and high strength. Electrolyte uptake, ionic conductivity and electrochemical stability window were measured by soaking the membranes into a liquid electrolyte consisting of 1 M lithium hexafluorophosphate ($LiPF_6$) dissolved in 1:1:1 (by volume) ethylene carbonate/dimethylcarbonate/ethylmethyl carbonate, and the results showed that electrospun PVDF-coated membrane had large electrolyte uptake capacity, high ionic conductivity and good electrochemical stability. The charge-discharge capacities and cycling performance were evaluated on Li/$LiFePO_4$ containing the as-prepared membranes as separators. It was demonstrated that the cell containing electrospun PVDF-coated PP nonwoven membrane had high capacity and good cycling performance. The Ramen spectra results showed that the electrospun PVDF-coated PP nonwoven membrane had good chemical stability.

5.1 Introduction

Lithium-ion battery are ubiquitous power source for portable electronics, hybrid vehicles and many other applications [88]. As one of the most critical components in lithium-ion batteries, separator plays an important role in keeping two electrodes apart and at the same time allowing the transportation of lithium ions freely [89]. This makes separator an important factor that affects the cycling performance and safety of lithium-ion batteries [89]. Polyethylene (PE), polypropylene (PP), and laminates of PE and PP, are the most widely used commercial polyolefin materials for producing lithium-ion battery separators with relatively thin thickness, good porosity, and small pore size (0.03–0.1 μm) and good electrochemical stability [89, 90]. However, polyolefin separators are not compatible with liquid electrolyte and their heat resistance is not sufficient which is a safety concern [89, 91].

Research efforts have been put on the improvement of lithium-ion battery separators. Examples of alternative separator membranes include but are not limited to the phase inversion membranes [92, 93], surface modified membranes [83, 94-95], sandwiched composite membranes [96], chemically modified membranes [97], and electrospun nanofiber membranes [84, 86].

Recently, nonwoven fabrics have been investigated for use as separators in lithium-ion batteries [73]. Their major advantages include low cost, high liquid electrolyte uptake and thermal stability [73]. However, nonwoven fabrics cannot be directly used in

lithium-ion batteries due to their large pose sizes and poor mechanical properties. The open pores formed by the microsized fibers in nonwoven fabrics are large, which lead to a serious battery safety concern. In addition, when the nonwoven fabrics are thin, they become mechanically weak and cannot withstand the tension force developed during the winding process of battery assembly.

One possible approach to modify nonwoven fabrics and make them into useful separators for lithium-ion batteries is to coat both sides of the nonwoven fabrics with nanofiber coatings prepared by electrospinning. Electrospun nanofiber coatings have controllable pore size and porosity, and improve the safety of the coated nonwoven membrane separators. The mechanical properties of nonwoven fabrics can also be improved by the electrospun nanofiber coatings.

Many polymers can be selected as the electrospinning material to produce nanofibers such as polyethylene oxide (PEO) [98-100], polycanbonate (PC) [101, 102], polyacrylonitrile (PAN) [103, 104], poly(methyl methacrylate) (PMMA) [105-107], and polyvinylidene fluoride (PVDF) [108-110]. Among these polymers, PVDF has good electrochemical stability and relatively high melting temperature and is suitable for producing electrospun nanofiber coatings on nonwoven fabrics.

This chapter uses the electrospinning approach as a coating method and PP nonwoven fabric as a substrate to produce electrospun PVDF-coated PP nonwoven membrane for use as the lithium-ion battery separator. After electrospinning, a hot-press process was used to reinforce the adhesion between the PVDF nanofiber layer and the PP nonwoven

substrate layer. The electrospun PVDF-coated PP nonwoven membrane was found to have better mechanical properties than uncoated nonwoven membrane. The PVDF nanofiber coating was also found to be able to enhance the wettability of the membranes and is beneficial to enhancing the ionic conductivity and cycling performance.

5.2 Experimental

5.2.1 Material

PVDF (O-Fluorine Chemical Technology, ShangHai, #904) with a molecular weight 600,000 g/mol, was used as the polymer to produce lithium-ion battery separator.

The solvent used was a mixture of N, N-dimethylformamide (DMF) (Sigma-Aldrich, ⩾99.8%) and acetone (Sigma-Aldrich, ⩾99.8%) with a ratio of 9:1 by volume. The liquid electrolyte consisted of 1 M lithium hexafluorophosphate ($LiPF_6$) dissolved in 1:1:1 (by volume) ethylene carbonate/dimethylcarbonate/ethylmethyl carbonate. The electrodes sued in cell performance were lithium metal electrodes (Sigma-Aldrich, 99.9%, 0.38mm thickness) and $LiFePO_4$ electrodes, consisting of active material $LiFePO_4$ (80wt.%, Hydro-Qubec), acetylene black (10 wt.%, Fisher Scientific) and polyvinylidene fluoride binder (10 wt.%, Aldrich).

5.2.2 Preparation of Electrospun PVDF-coated PP Nonwoven membrane

Electrospinning polymer solution (10 wt%) was prepared by using the mixture solvent of N,N-dimethylformamide (DMF) (Sigma-Aldrich, ⩾99.8%) and acetone (Sigma-Aldrich,

≥99.8%) with a ratio of 9:1 by volume. Liquid electrolyte is made of 1 M lithium hexafluorophosphate (LiPF6) dissolved in 1:1:1 (by volume) ethylene carbonate/dimethylcarbonate/ethylmethyl carbonate.

After preparing the PVDF solution, it was mechanically stirred under room temperature for 24 h before electrospinning. At first, one side of the PP nonwoven fabric was attached to the collector and the electrospinning was processed on the other side. After specific time of electrospinning with the parameter of 15kV, distance between needle and collector 15cm and flow rate 0.8 ml/h, the PVDF nanofibers were deposited on the surface of the PP nonwoven substrate. After accumulation of the nanofibers for specific time on one side of the substrate, the nonwoven fabric was turned over and the same process was processed for same period.

When the electrospinning-coating process was done, the composite membrane was hot-pressed under 100 ℃, 500spi for 10min to strengthen the adhesion between the electrospun PVDF coating layer and the PP nonwoven substrate. The entire electrospinning and hot-press treatment is shown in Figure 5.1.

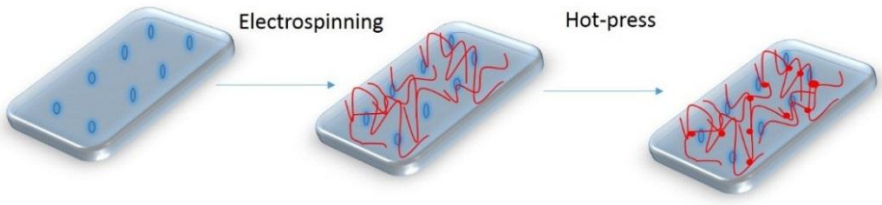

Figure 5.1 Schematic of the experimental process.

5.2.3 Structure characterization and property measurements

The morphology of electrospun PVDF-coated PP nonwoven membrane was investigated using a scanning electron microscopy (JEOL 6400F Field emission SEM) with an acceleration voltage of 20 kV. In order to reduce charging, the PVDF membranes were coated with Au by a K-550X sputter coater prior to the SEM observation. The nanofiber diameter data was obtained by measuring fifty fibers randomly selected in SEM images using Revolution v1.6.0 software.

Electrolyte uptake test was conducted by soaking pre-weighted separator membranes into a liquid electrolyte for a specific time at room temperature in the glove box filled with protecting argon gas. The electrolyte used for the test consists of 1 M lithium hexafluorophosphate ($LiPF_6$) dissolved in 1:1:1 (by volume) ethylene carbonate/dimethylcarbonate/ethylmethyl carbonate. The soaked membrane was weighted again after removing the excess electrolyte solution adhering to the separator membrane by gently wiping with filter paper. The electrolyte uptake was calculated by:

$$\textit{Electrolyte Uptake}\ (\%) = (W_f - W_0)/W_0 \times 100 \qquad (5.1)$$

where W_f and W_0 are the weights of the electrolyte-soaked membranes and dry membranes, respectively.

The mechanical properties of hot-pressed electrospun PVDF membrane, electrospun PVDF-coated PP nonwoven membrane, and PP nonwoven fabric were measured using the same machine in the Chapter 4. Before each sample was tested, the membranes were cut into 1cm × 5cm size and the thickness of the membranes were measured and recorded.

In the process of the tensile test, the upper clip moved up at a constant rate until the sample broke.

The ionic conductivities of the electrolyte-soaked membranes were measured by electrochemical impedance spectroscopy (EIS) using Reference 600 Potentiostat/Galvanostat/ZRA (GAMRY). Before the measurement, the electrolyte-soaked membranes were sandwiched between two symmetrical stainless-steel plate electrodes and sealed in an argon-filled glove box. The measurement was performed with the amplitude of 10mV over a frequency range of 1000 kHz to 1Hz at a temperature range between 25 and 85 ℃. The intercept on the real-axis of the Nyquist plot gave the resistance R_b of the membrane soaked in the liquid electrolyte under different temperatures. The ionic conductivity (σ) was calculated by following equation:

$$\sigma = d / (R_b \times A) \tag{5.2}$$

where d is the membrane thickness, R_b the bulk resistance of liquid electrolyte-soaked membrane, and A is the cross-sectional area of the membrane.

The electrochemical stability windows of the liquid electrolyte-soaked electrospun PVDF membrane, electrospun PVDF-coated PP nonwoven membrane and Celgard membrane were performed by linear sweep voltammetry using the Reference 600 Potentiostat/Galvanostat/ZRA (GAMRY) under the scan rate of $10mVs^{-1}$ and the potential range from 2.5V to 6V at room temperature.

The electrochemical performance of lithium/lithium iron phosphate ($LiFePO_4$) cells with liquid electrolyte-soaked membranes as separators was studied The batteries were

assembled by sandwiching the liquid electrolyte-soaked membrane between the lithium and $LiFePO_4$ electrodes and charge and discharge cycles were conducted using an Arbin automatic battery tester in the potential window of 2.5 - 4.2 V at 0.2 C rate.

Raman spectra was used to evaluate the chemical stability of the electrospun PVDF-coated PP nonwoven membrane after 40 charge-discharge cycles. The electrospun PVDF-coated PP nonwoven was tested before assembling into the coin cells and after 40 charge-discharge cycles, the separator was taken out of the coin cell and cleaned completely with ethanol and deionized water. After drying in the vacuum for 24 hours, it was tested again with the Raman spectra.

5.3 Result and Discussion

5.3.1 SEM images

Figures 5.2 and 5.3 show the SEM images of PP nonwoven fabric substrate and electrospun PVDF-coated PP nonwoven membrane. As shown Figure 5.2, the PP nonwoven fabric has much large fiber diameter (around 20 μm) and very smooth fiber surface. The pore size of the nonwoven fabric is greater than 100 μm, which is too large for lithium-ion battery separator application. From Figure 5.3, it is seen that the deposition of electrospun PVDF nanofibers lead to the formation of a nanofiber layer with significantly smaller diameter (around 180 nm) and pore size (a few micrometers) on the surface of the PP nonwoven membrane (Figure 5.3). The smaller fiber diameter and pore size improve the cell safety by avoiding the penetration of microsized electrode

particles.

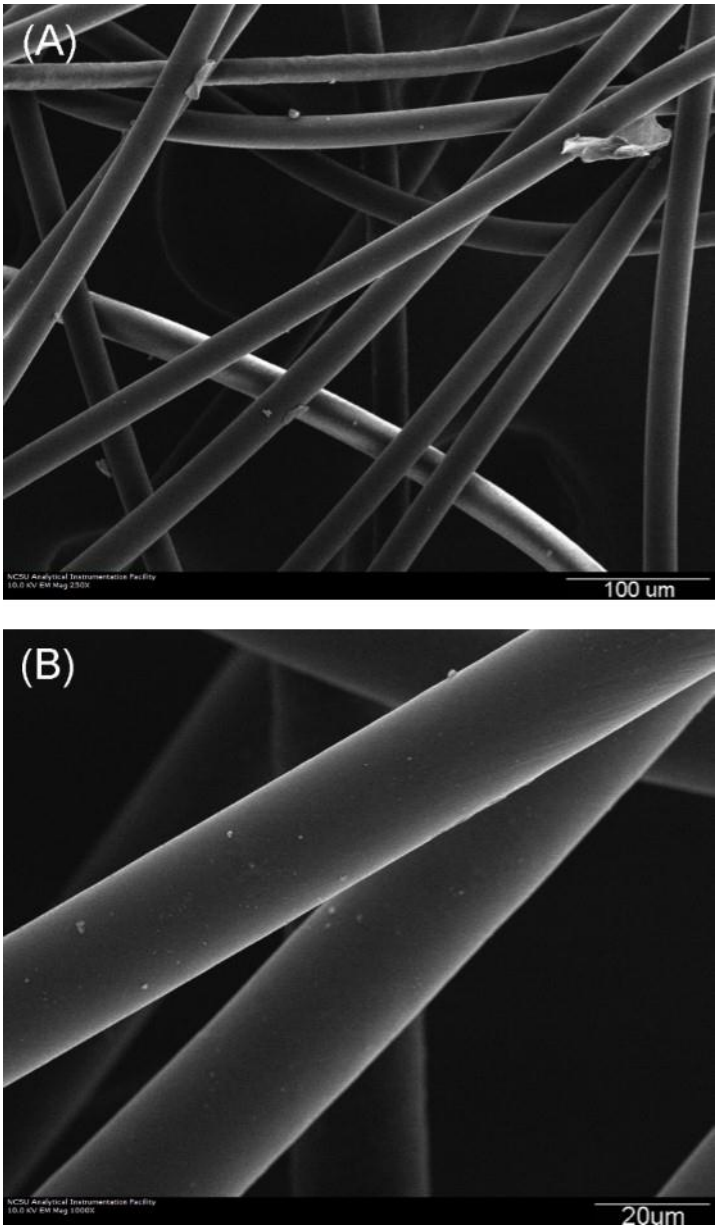

Figure 5.2 SEM images of PP nonwoven substrate.

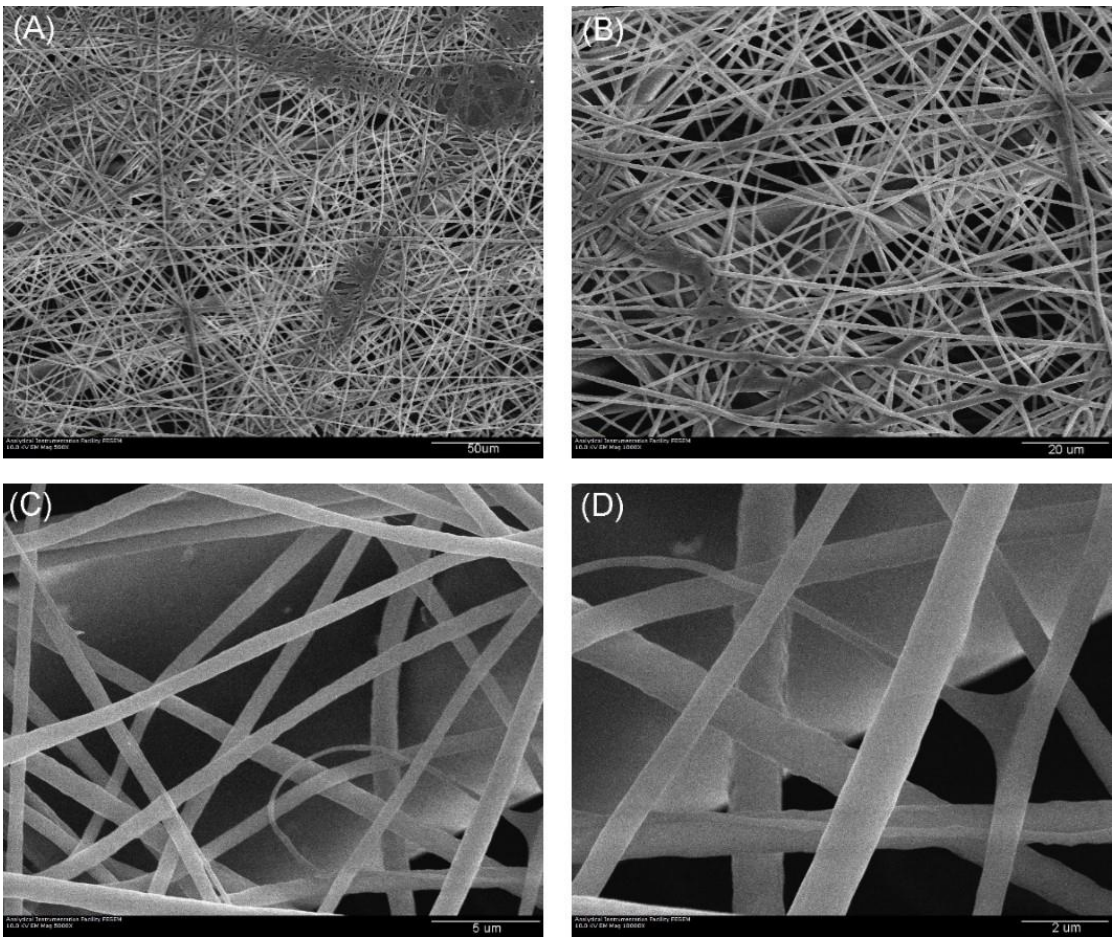

Figure 5.3 SEM images of electrospun PVDF-coated PP nonwoven membranes.

5.3.2 Tensile properties

One of the most important requirements during battery assemble process is the tensile strength and the separator should be strong enough to withstand winding force during cell winding and assembly [57].

Table 5.1 Average tensile strength, modulus, and strain-at-break of PP nonwoven fabric, electrospun PVDF membrane (hot-pressed), and electrospun PVDF-coated PP nonwoven membrane

	Tensile strength (MPa)	Modulus (MPa)	Strain-at-break (mm/mm)
PP nonwoven fabric (Machine direction)	2.5	44.3	2.53
Electrospun PVDF membrane	4.1	203.1	0.07
Electrospun PVDF-coated PP nonwoven membrane (Machine direction)	3.9	241.7	2.96

Table 5.1shows the tensile strength, modulus and strain-at-break of PP nonwoven fabric and electrospun PVDF-coated PP nonwoven membrane. For comparison, the tensile properties of free-standing electrospun PVDF nanofiber membranes are also shown. From Table 5.1, it is seen that electrospun PVDF-coated PP nonwoven membrane has significantly higher strength and higher modulus than the uncoated PP nonwoven

membrane. The strength and modulus of electrospun PVDF-coated PP nonwoven membrane are comparable to those of electrospun PVDF membrane. The strain-at-break of electrospun PVDF-coated PP nonwoven membrane is between those of PP nonwoven fabric and electrospun PVDF membrane. Results demonstrated that coating electrospun PVDF nanofibers can improve the mechanical properties of PP nonwoven fabric.

5.3.3 Electrolyte Uptake

Electrolyte uptake is an important property parameter indicating the ability of separator membrane to absorb and maintain liquid electrolyte. During battery assembly, the separator must have the ability to be wetted completely and quickly by the typical liquid electrolyte [57]. A separator with poor wettability limits the performance of the battery by increasing the cell resistance [57].

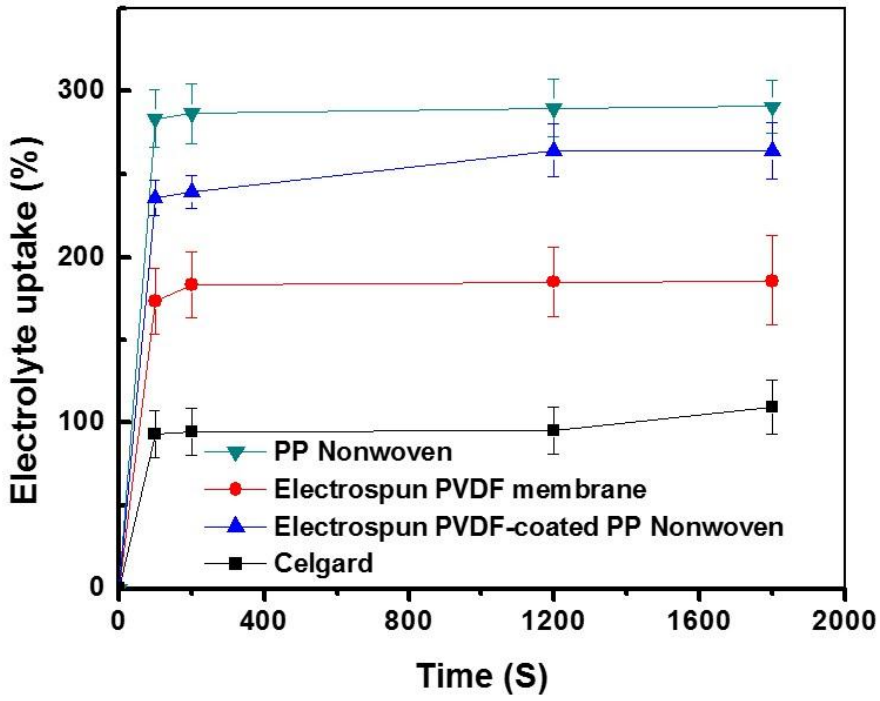

Figure 5.4 Electrolyte uptakes as a function of time for Celgard, PP nonwoven, electrospun PVDF, and electrospun PVDF-coated PP nonwoven.

Figure 5.4 shows the electrolyte uptakes of Celgard, PP nonwoven, electrospun PVDF, and electrospun PVDF-coated PP nonwoven membranes. All four membranes absorb liquid electrolyte quickly and reach saturated electrolyte uptakes in 200s. The Celgard membrane is made of PE and has the lowest electrolyte uptake due to the absence of polar groups on its polymer backbone and relatively low porosity. The PP nonwoven membrane has significantly greater electrolyte uptakes than other membranes due to its high porosity and large pore size. Electrospun PVDF and electrospun PVDF-coated PP nonwoven membranes also have relatively high electrolyte uptakes partially because of the presence of polar groups on the polymer backbones of PVDF and the increased surface areas

Although the electrolyte uptakes of electrospun PVDF and electrospun PVDF-coated PP nonwoven membranes are lower than those of PP nonwoven, they are significantly greater than those of Celgard membrane are sufficient for practical lithium-ion battery application..

5.3.4 Ionic Conductivity

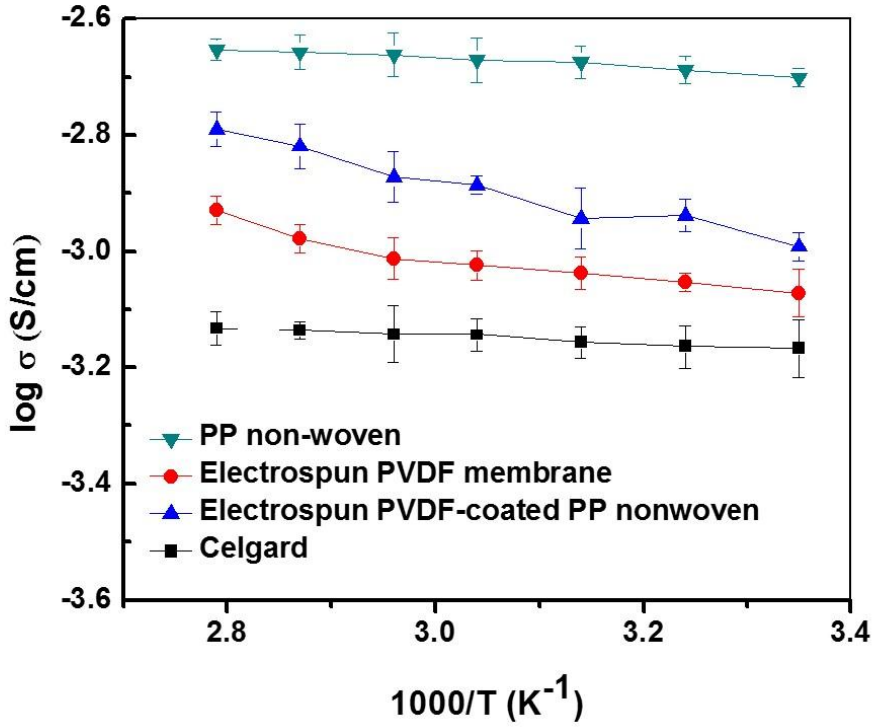

Figure 5.5 Ionic conductivities of liquid electrolyte-soaked membranes at various temperatures.

The ionic conductivity of liquid electrolyte-soaked separator membrane is a function of the conductivity of the liquid electrolyte, and the porosity and, tortuosity of the liquid electrolyte-soaked membrane [114]. Figure 5.5 shows the ionic conductivities of liquid electrolyte-soaked Celgard, PP nonwoven, electrospun PVDF, and electrospun PVDF-coated PP nonwoven membranes. For these four membranes, the ionic

conductivities increase as the temperature increases due to the enhanced mobility of ions at higher temperatures [113].

As shown in Figure 5.5, PP nonwoven fabric has the highest ionic conductivities under all temperatures since it can absorb the largest amount of electrolyte in its large pores. Electrospun PVDF-coated PP nonwoven membrane has the second highest ionic conductivities. Compared with the electrospun PVDF-coated PP nonwoven membrane, the electrospun PVDF membrane has lower ionic conductivity after absorbing liquid electrolyte mainly because it has lower electrolyte uptake capacity.

5.3.5 Electrochemical Stability Window

Kinetic electrochemical stability window is another important parameter in evaluating the performance of lithium-ion battery separators. The onset of a steady increase in the voltage under specific current density corresponds to the anodic stability limit of the liquid electrolyte-soaked membrane [115-117]. In general, the electrochemical stability window of liquid electrolyte-soaked separator membrane is mainly determined by the stability of the liquid electrolyte. However, the use of electrochemically-unstable separator could reduce the stability window of liquid electrolyte-soaked separator membrane.

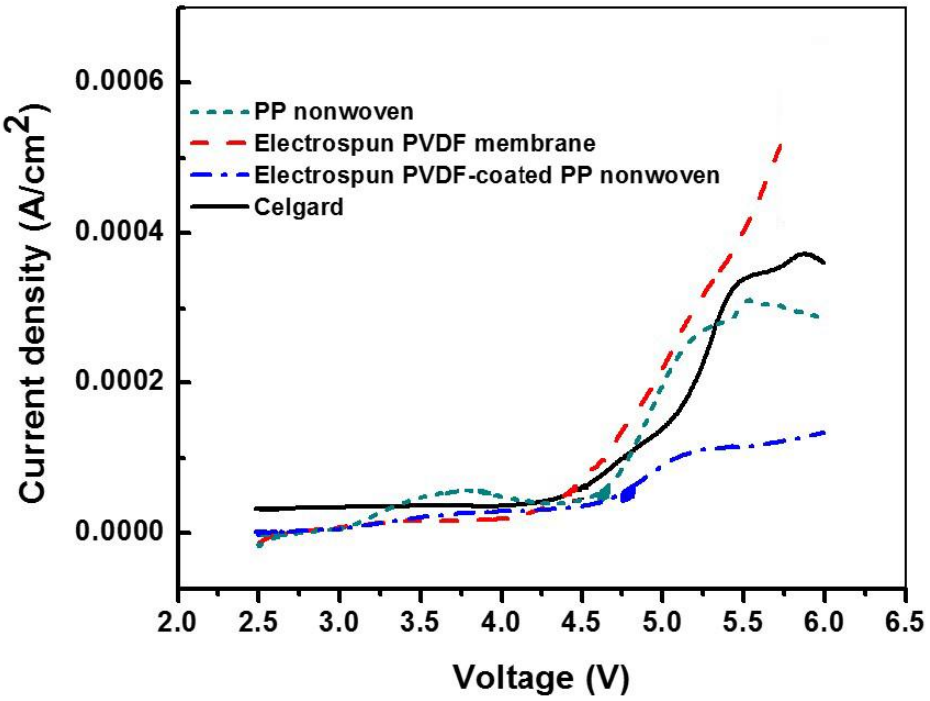

Figure 5.6 Electrochemical stability windows of liquid electrolyte-soaked Celgard, PP non-woven fabric, electrospun PVDF-coated PP nonwoven membranes.

Figure 5.6 shows the electrochemical stability windows of the liquid electrolyte-soaked membranes. Among all four membranes, liquid electrolyte-soaked electrospun PVDF-coated PP nonwoven membrane has the highest electrochemical stability window of around 4.8V, which is higher than the operational voltage of most cathode materials.

The results demonstrate that the electrospun PVDF-coated PP nonwoven membrane can be used with most high-voltage cathode materials in rechargeable lithium-ion batteries.

5.3.6 Cell Performance

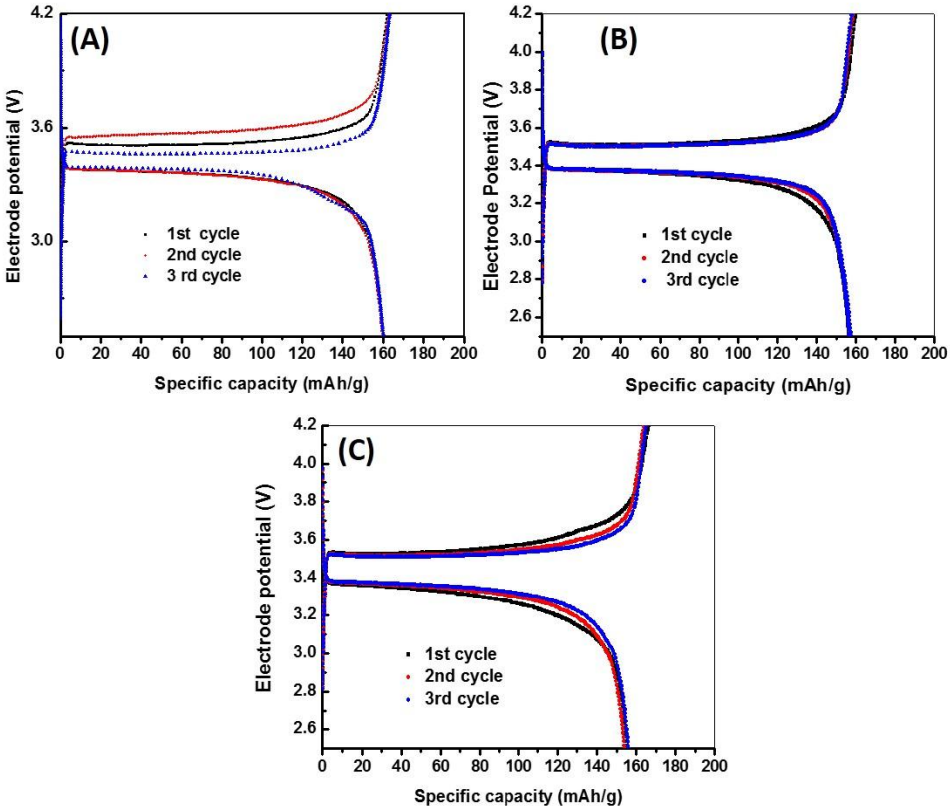

Figure 5.7 Charge-discharge curves of Li/$LiFePO_4$ cells containing: (A) Celgard, (B) electrospun PVDF, and (C) electrospun PVDF-coated PP nonwoven membrane.

Figure 5.7 shows the charge-discharge curves of the first three cycles of the Li/$LiFePO_4$ cells using Celgard, electrospun PVDF, and electrospun PVDF-coated PP nonwoven membranes. It is seen that the three cells with different membrane separators show initial discharge capacities of 161, 159, and 155 mAh/g respectively. Considering the theoretical capacity of $LiFePO_4$ (170 mAh/g), the charge-discharge capacities of these cells are satisfactory.

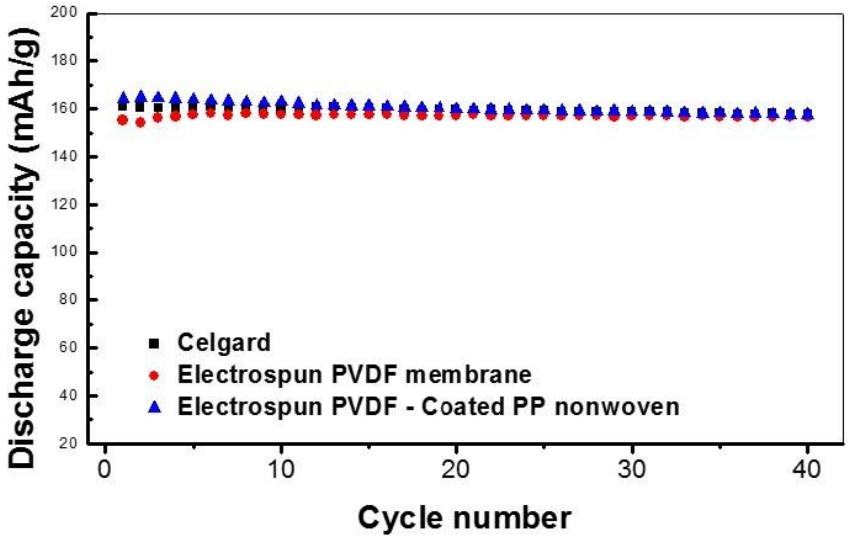

Figure 5.8 Cycle performance of Li/$LiFePO_4$ cells containing Celgard, electrospun PVDF membrane, and electrospun PVDF-coated PP nonwoven membranes.

The cycling performance of Li/$LiFePO_4$ cells contacting Celgard, electrospun PVDF, and electrospun PVDF-coated PP nonwoven membranes is shown in Figure 5.8. At the 40^{th} cycle, the cells show discharge capacities 165, 157, and 156 mAh/g. Therefore, all the three membranes show good charge-discharge stability during cycling.

5.3.7 Raman spectra

Figure 5.9 compares the Raman spectra of electrospun PVDF-coated PP nonwoven membrane before and after 40 cycles. Characteristic peaks of PVDF are shown at 1429, 1211, 1073, 973, and 762 cm^{-1}. There are no changes in peak positions or intensities after 40 cycles. Therefore, the chemical structure of electrospun PVDF-coated PP nonwoven membrane is very stable during cycling. The results indicate electrospun PVDF-coated PP nonwoven membrane is a promising separator cathode for use in lithium-ion batteries.

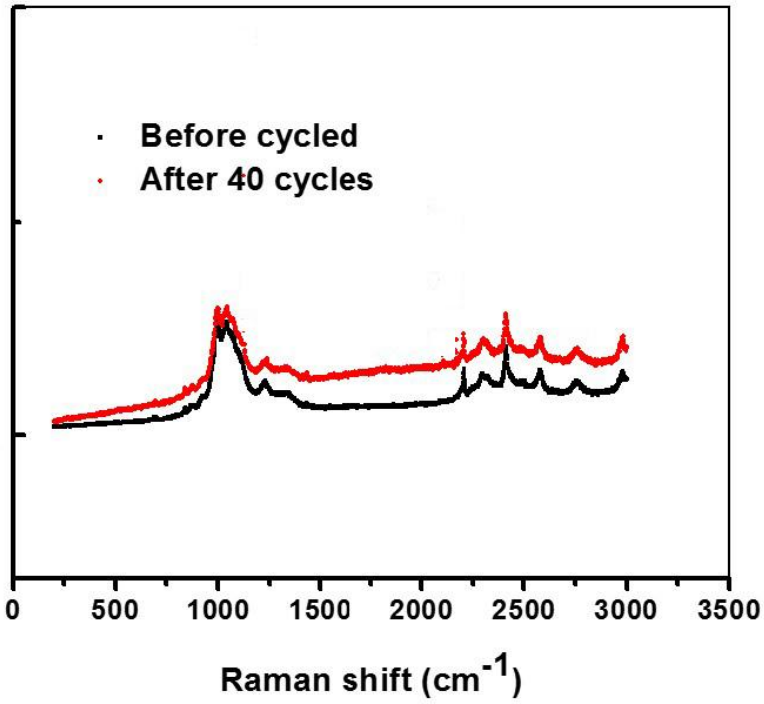

Figure 5.9 Raman spectra of electrospun PVDF-coated PP nonwoven membrane before and after cycling.

5.4 Conclusion

Electrospun PVDF coated PP nonwoven composite membrane was prepared by electrospinning, followed by a hot press process. The PVDF nanofibers were dispersed uniformly on the surface of the PP non-woven substrate. After hot-press, the tensile strength, modulus, and strain-at-break are adequate to withstand the winding force need for assembling lithium-ion batteries. In addition, electrospun PVDF-coated PP nonwoven membrane has large electrolyte uptake capacity and exhibit high ionic conductivity after being soaked in a liquid electrolyte. Electrospun PVDF-coated PP nonwoven membrane

also presents good electrochemical and chemical stability and Li/LiFeP4 cells using the membrane has good cycling performance. It is, therefore, demonstrated that electrospun PVDF-coated PP nonwoven membrane is acceptable as lithium-ion battery separator.

Chapter 6 Conclusion

This research concentrates on the fabrication and characterization of electrospun polyvinylidene fluoride (PVDF) nanofiber membranes and electrospun PVDF-coated PP nonwoven membranes. The major results and conclusion are summarized as follows.

(1) Electrospun PVDF nanofiber membranes with different applied voltages for use as lithium-ion battery separators.

Electrospun PVDF nanofiber membranes were prepared under different applied voltages. For the membranes prepared under 15kV, the effect of hot-press treatment was studied.

The morphology of nanofiber membranes was studied by the SEM images and it was found that the membrane prepared at 15 kV was more uniform than the other two. Electrolyte uptake test was processed by soaking pre-weighted separator membranes into a liquid electrolyte which consisted of 1 M lithium hexafluorophosphate ($LiPF_6$) dissolved in 1:1:1 (by volume) ethylene carbonate/dimethylcarbonate/ethylmethyl carbonate for a specific time at room temperature in a glove box filled with protecting argon gas. The results showed that hot-press treatment decreased the electrolyte capacity of nanofiber membrane by decreasing the membrane porosity.

The ionic conductivities of PVDF nanofiber membranes with different applied voltages were measured by sandwiching the electrolyte-soaked membranes between two symmetrical stainless-steel plate electrodes and sealed in argon-filled glove box. The

results showed that the applied voltage have limited effects on the ionic conductivity and hot-pressed membrane had a reduced ionic conductivity due to its lower electrolyte uptake capacity.

The cell performance was tested by assembling coin-type Li/$LiFePO_4$ cells using electrospun PVDF membranes as the separator. The results showed that hot-press did not have negative effect on the cycling stability of the cells. On the contrary, it made the charge-discharge process more stable and increased the electrochemical stability. The results indicate that electrospun PVDF membranes have great potential to be used as lithium-ion battery separators.

(2) Electrospun PVDF-Coated Nonwoven Polypropylene as Lithium-ion Battery Separators.

The composite membrane was prepared by electrospinning with PP nonwoven substrate adhered to the collector. Both sides of the PP nonwoven fabric substrate were coated. In order to strengthen the adhesion strength between electrospun PVDF coating layer and PP non-woven substrate, hot-press treatment was applied after electrospinning step.

The morphology of the composite membrane was studied by SEM images. Electrolyte uptake test was processed by soaking pre-weighted separator membranes into the electrolyte for a specific time at room temperature in the glove box filled with protecting argon gas. The results showed that the composite membrane had a higher electrolyte uptake capacity and ionic conductivity than the electrospun PVDF and the

Cellgard membrane due to its higher porosity and increased capillarity force.

In order to evaluate the electrochemical cell performance, coin cells were assembled with Li/$LiFePO_4$ electrodes. The results showed that the cycling stability was good when the composite membranes were used as separators. Besides, the chemical stability of composite membrane was evaluated using Raman spectra before and after 40 cycles. The results showed good chemical stability for the composite membrane when soaked in the liquid electrolyte for a long time after 40 charge-discharge cycles.

Chapter 7 Recommendation work

In order to further improve the properties of the membrane separators, the recommended work is represented as follows.

(1) Surface modification of the composite membranes.

In order to improve the wettability of the polyolefin substrate, some surface modification methods such plasma can be applied on the surface of the PP nonwoven fabric. Recently, research efforts have concentrated on the surface modification of the polyolefin membranes to improve their wettability [95, 118]. The plasma-induced coating process and gamma ray were utilized and the wettability, thermal stability and electrochemical properties were improved by these methods. Therefore, applying specific surface modification method can potentially bring positive effects on the performance of the separators.

(2) Incorporation of specific inorganic particles into the electrospun nanofibers.

Adding inorganic particles, such as TiO_2, and SiO_2, into the separator membranes can increase the thermal stability and wettability [85, 119]. Electrospun nanofiber membranes containing inorganic particles can be obtained using normal electrospinning method and the particle content can be controlled. The effect of different contents of inorganic particles on the performance of the membrane separators should be studied. It is anticipated that the incorporation of the inorganic particles can improve the electrochemical properties.

References

[1] Pavlov, D. (2011). *: Science and technology* Elsevier Science.

[2] A. Volta, “On the electricity excited by the mere contact of conducting substances of different kinds,” Philosophical Transactions, pp. 403-431, 1800.

[3] Scrosati, B. (2011). History of lithium batteries. *Journal of Solid State Electrochemistry, 15*(7), 1623-1630. doi: 10.1007/s10008-011-1386-8

[4] Battery. (2 February 2013). Retrieved 02/06, 2013, from http://en.wikipedia.org/wiki/Battery_(electricity)#Battery_cell_types

[5] Palac ń, M. R. (2009). Recent advances in rechargeable battery materials: A chemist's perspective. *Chemical Society Reviews,38*(9), 2565.

[6] Thackeray, M. M., Wolverton, C., & Isaacs, E. D. (2012). Electrical energy storage for transportation-approaching the limits of, and going beyond, lithium-ion batteries. *Energy & Environmental Science, 5*(7), 7854-7863. doi: 10.1039/c2ee21892e

[7] Battery Technology Handbook H . A . Kiehne CRC Press 2003 Print ISBN: 978-0-8247-4249-2 eBook ISBN: 978-0-203-91185-3 DOI: 10.1201/9780203911853.ch1

[8] History of the battery. (2013). Retrieved 02/06, 2013, from http://en.wikipedia.org/wiki/History_of_the_battery

[9] Nickel–iron battery. (2013). Retrieved 02/06, 2013, from http://en.wikipedia.org/wiki/Nickel-iron_battery#Durability

[10] Dunn, B., Kamath, H., & Tarascon, J. (2011). Electrical energy storage for the grid: A battery of choices. *Science (New York, N.Y.), 334*(6058), 928.

[11] Min Yang, & Junbo Hou. (2012). Membranes in lithium ion batteries. *Membranes, 2*(3), 367-383.

[12] Jeong, G., Kim, Y., Kim, H., Kim, Y., & Sohn, H. (2011). Prospective materials and applications for li secondary batteries. *Energy & Environmental Science, 4*(6), 1986. doi: 10.1039/c0ee00831a

[13] Tarascon, J. M., & Armand, M. (2001). Issues and challenges facing rechargeable lithium batteries. *Nature, 414*(6861), 359-367. doi: 10.1038/35104644

[14] Nishi, Y. (2001). The development of lithium ion secondary batteries. *Chemical Record (New York, N.Y.), 1*(5), 406-413. doi: 10.1002/tcr.1024

[15] Yoshino, A. (2012). The birth of the lithium-ion battery.*Angewandte Chemie (International Ed. in English), 51*(24), 5798-5800. doi: 10.1002/anie.201105006

[16] Lewis, H., Park, H., & Paolini, M. (2012). Frontier battery development for hybrid vehicles. *Chemistry Central Journal, 6 Suppl 1*(Suppl 1), S2-S2. doi: 10.1186/1752-153X-6-S1-S2

[17] Fontaine, P. J. (2008). Shortening the path to energy independence: A policy agenda to commercialize Battery–Electric vehicles. *The Electricity Journal, 21*(6), 22-42. doi: 10.1016/j.tej.2008.07.006

[18] Inaba, M., & Ogumi, Z. (2001). Up-to-date development of lithium-ion batteries in japan. *Ieee Electrical Insulation Magazine, 17*(6), 6-20.

[19] Mikolajczak, C., Kahn, M., White, K., & Long, R. T. (2012).*Lithium-ion batteries hazard and use assessment*. New York: Springer New York.

[20] Whittingham, M. S. (2004). Lithium batteries and cathode materials. *Chemical Reviews, 104*(10), 4271.

[21] Fergus, J. W. (2010). Recent developments in cathode materials for lithium ion batteries. *Journal of Power Sources, 195*(4), 939-954. doi: 10.1016/j.jpowsour.2009.08.089

[22] Mizushima, K., Jones, P. C., Wiseman, P. J., & Goodenough, J. B. (1980). Li xCoO 2 (0<x<-1): A new cathode material for batteries of high energy density. *Materials Research Bulletin,15*(6), 783-789. doi: 10.1016/0025-5408(80)90012-4

[23] Issue and challenges facing rechargeable thin film lithium batteries. (2008). *Materials Research Bulletin, 43*(8), 1913-1942. doi: 10.1016/j.materresbull.2007.08.031

[24] Akimoto, J., Gotoh, Y., & Oosawa, Y. (1998). Synthesis and structure refinement of $LiCoO_2$Single crystals. *Journal of Solid State Chemistry, 141*(1), 298-302. doi: 10.1006/jssc.1998.7966

[25] OZAWA, K. (1994). Lithium-ion rechargeable batteries with $LiCoO_2$ and carbon electrodes: The $LiCoO_2$/C system. *Solid State Ionics, 69*(3-4), 212-221. doi: 10.1016/0167-2738(94)90411-1

[26] Fergus, J. W. (2010). Recent developments in cathode materials for lithium ion batteries. *Journal of Power Sources, 195*(4), 939-954. doi: 10.1016/j.jpowsour.2009.08.089

[27] Synthesis and structural characterization of defect spinels in the lithium-manganese-oxide system. (1993). *Materials Research Bulletin, 28*(10), 1041-1049. doi: 10.1016/0025-5408(93)90142-Z

[28] Aurbach, D., Levi, M. D., Gamulski, K., Markovsky, B., Salitra, G., Levi, E., . . . Oesten, R. (1999). Capacity fading of LixMn2O4 spinel electrodes studied by XRD and electroanalytical techniques. *Journal of Power Sources, 81-82*, 472-479. doi: 10.1016/S0378-7753(99)00204-9

[29] Lai, C., Xu, Q., Ge, H., Zhou, G., & Xie, J. (2008). Improved electrochemical performance of LiFePO4/C for lithium-ion batteries with two kinds of carbon sources. *Solid State Ionics,179*(27-32), 1736-1739. doi: 10.1016/j.ssi.2008.03.042

[30] Salah, A., Mauger, A., Julien, C., & Gendron, F. (2006). Nano-sized impurity phases in relation to the mode of preparation of LiFePO4. *Materials Science and Engineering b-Solid State Materials for Advanced Technology, 129*(1-3), 232-244. doi: 10.1016/j.mseb.2006.01.022

[31] Tang, K., Sun, J., Yu, X., Li, H., & Huang, X. (2009). Electrochemical performance of LiFePO4 thin films with different morphology and crystallinity. *Electrochimica Acta,54*(26), 6565-6569. doi: 10.1016/j.electacta.2009.06.030

[32] Islam, M., Driscoll, D., Fisher, C., & Slater, P. (2005). Atomic-scale investigation of defects, dopants, and lithium transport in the LiFePO4 olivine-type battery material. *Chemistry of Materials, 17*(20), 5085-5092. doi: 10.1021/cm050999v

[33] Zhang, Y., Huo, Q., Du, P., Wang, L., Zhang, A., Song, Y., . . . Li, G. (2012). Advances in new cathode material LiFePO4 for lithium-ion batteries. *Synthetic Metals, 162*(13-14), 1315-1326. doi: 10.1016/j.synthmet.2012.04.025

[34] Dong, Y., Zhao, Y., Chen, Y., He, Z., & Kuang, Q. (2009). Optimized carbon-coated LiFePO4 cathode material for lithium-ion batteries. *Materials Chemistry and Physics, 115*(1), 245-250. doi: 10.1016/j.matchemphys.2008.11.063

[35] Park, K., Son, J., Chung, H., Kim, S., Lee, C., & Kim, H. (2003). Synthesis of LiFePO4 by co-precipitation and microwave heating. *Electrochemistry Communications, 5*(10), 839-842. doi: 10.1016/j.elecom.2003.08.005

[36] Yuan, X., Liu, H., & Zhang, J. (2012). *Lithium-ion batteries: Advanced materials and technologies*. Boca Raton: CRC Press.

[37] Wu, Y. P., Rahm, E., & Holze, R. (2003). Carbon anode materials for lithium ion batteries. *Journal of Power Sources, 114*(2), 228-236. doi: 10.1016/S0378-7753(02)00596-7

[38] Endo, M., Kim, C., Nishimura, K., Fujino, T., & Miyashita, K. (2000). Recent development of carbon materials for li ion batteries. *Carbon, 38*(2), 183-197. doi: 10.1016/S0008-6223(99)00141-4

[39] Li, H., Wang, Z., Chen, L., & Huang, X. (2009). Research on advanced materials for li-ion batteries. *Advanced Materials,21*(45), 4593-4607. doi: 10.1002/adma.200901710

[40] Szczech, J. R., & Jin, S. (2010). Nanostructured silicon for high capacity lithium battery anodes. *Energy & Environmental Science, 4*(1), 56. doi: 10.1039/c0ee00281j

[41] Peled, E. (1996). Improved graphite anode for lithium-ion batteries chemically. *Journal of the Electrochemical Society,143*(1), L4. doi: 10.1149/1.1836372

[42] Idota, Y., Kubota, T., Matsufuji, A., Maekawa, Y., & Miyasaka, T. (1997). Tin-based amorphous oxide: A high-capacity lithium-ion-storage material. *Science, 276*(5317), 1395-1397. doi: 10.1126/science.276.5317.1395

[43] Han, S., Jang, B., Kim, T., Oh, S., & Hyeon, T. (2005). Simple synthesis of hollow tin dioxide microspheres and their application to lithium-ion battery anodes. *Advanced Functional Materials, 15*(11), 1845-1850. doi: 10.1002/adfm.200500243

[44] Winter, M., Besenhard, J. O., Spahr, M. E., & Novák, P. (1998). Insertion electrode materials for rechargeable lithium batteries.*Advanced Materials, 10*(10), 725-763. doi: 10.1002/(SICI)1521-4095(199807)10:10<725::AID-ADMA725>3.0.CO;2-Z

[45] Yang, J., Winter, M., & Besenhard, J. O. (1996). Small particle size multiphase li-alloy anodes for lithium-ionbatteries. *Solid State Ionics, 90*(1), 281-287. doi: 10.1016/S0167-2738(96)00389-X

[46] Li, H. (1999). A high capacity nano-si composite anode material for lithium rechargeable batteries. *Electrochemical and Solid-State Letters, 2*(11), 547. doi: 10.1149/1.1390899

[47] Li, H., Huang, X., Chen, L., Zhou, G., Zhang, Z., Yu, D., . . . Pei, N. (2000). The crystal structural evolution of nano-si anode caused by lithium insertion and extraction at

room temperature.*Solid State Ionics, 135*(1), 181-191. doi: 10.1016/S0167-2738(00)00362-3

[48] Poizot, P., Laruelle, S., Grugeon, S., Dupont, L., & Tarascon, J. M. (2000). Nano-sized transition-metal oxides as negative-electrode materials for lithium-ion batteries. *Nature, 407*(6803), 496-499. doi: 10.1038/35035045

[49] Li, H., Balaya, P., & Maier, J. (2004). Li-storage via heterogeneous reaction in selected binary metal fluorides and oxides. *Journal of the Electrochemical Society, 151*(11), A1878. doi: 10.1149/1.1801451

[50] Hayner, C. M., Zhao, X., & Kung, H. H. (2012). Materials for rechargeable lithium-ion batteries. *Annual Review of Chemical and Biomolecular Engineering, 3*(1), 445-471. doi: 10.1146/annurev-chembioeng-062011-081024

[51] Larcher, D., Beattie, S., Morcrette, M., Edström, K., Jumas, J., Tarascon, J., . . . Teknisk-naturvetenskapliga vetenskapsområdet. (2007). Recent findings and prospects in the field of pure metals as negative electrodes for li-ion batteries. *Journal of Materials Chemistry, 17*(36), 3759. doi: 10.1039/b705421c

[52] Song, J. Y., Wang, Y. Y., & Wan, C. C. (1999). Review of gel-type polymer electrolytes for lithium-ion batteries. *Journal of Power Sources, 77*(2), 183-197. doi: 10.1016/S0378-7753(98)00193-1

[53] Fergus, J. W. (2010). Ceramic and polymeric solid electrolytes for lithium-ion batteries. *Journal of Power Sources, 195*(15), 4554-4569. doi: 10.1016/j.jpowsour.2010.01.076

[54] Tatsumisago, M., Mizuno, F., & Hayashi, A. (2006). All-solid-state lithium secondary batteries using sulfide-based glass–ceramic electrolytes. *Journal of Power Sources, 159*(1), 193-199. doi: 10.1016/j.jpowsour.2006.04.037

[55] Minami, T., Hayashi, A., & Tatsumisago, M. (2006). Recent progress of glass and glass-ceramics as solid electrolytes for lithium secondary batteries. *Solid State Ionics, 177*(26), 2715-2720. doi: 10.1016/j.ssi.2006.07.017

[56] Minami, K., Hayashi, A., Ujiie, S., & Tatsumisago, M. (2009). Structure and properties of Li2S–P2S5–P2S3 glass and glass–ceramic electrolytes. *Journal of Power Sources,189*(1), 651-654. doi: 10.1016/j.jpowsour.2008.09.044

[57] Arora, P., & Zhang, Z. J. (2004). Battery separators. *Chemical Reviews, 104*(10), 4419-4462. doi: 10.1021/cr020738u

[58] Huang, X. (2011). Separator technologies for lithium-ion batteries. *Journal of Solid State Electrochemistry, 15*(4), 649-662. doi: 10.1007/s10008-010-1264-9

[59] Lee, Y. M., Lee, J. A., Kim, J., Choi, N., Seol, W., & Park, J. (2005). Novel porous separator based on PVdF and PE non-woven matrix for rechargeable lithium batteries. *Journal of Power Sources, 139*(1), 235-241. doi: 10.1016/j.jpowsour.2004.06.055

[60] Sohn, J., Im, J., Shin, J., & Nho, Y. (2012). PVDF-HFP/PMMA-coated PE separator for lithium ion battery. *Journal of Solid State Electrochemistry, 16*(2), 551-556. doi: 10.1007/s10008-011-1379-7

[61] Tabatabaei, S. H., Carreau, P. J., & Ajji, A. (2009). Microporous membranes obtained from PP/HDPE multilayer films by stretching. *Journal of Membrane Science, 345*(1), 148-159. doi: 10.1016/j.memsci.2009.08.038

[62] Takita, K.; kono, K.; Takashima, T.; Okamoto, K. U.S. Patent, 5,051,183, 1991.

[63] Ihm, D., Noh, J., & Kim, J. (2002). Effect of polymer blending and drawing conditions on properties of polyethylene separator prepared for li-ion secondary battery. *Journal of Power Sources, 109*(2), 388-393. doi: 10.1016/S0378-7753(02)00097-6

[64] Teo, W. E., & Ramakrishna, S. (2006). A review on electrospinning design and nanofibre assemblies.*Nanotechnology, 17*(14), R89-R106. doi: 10.1088/0957-4484/17/14/R01

[65] Huang, Z., Zhang, Y. -., Kotaki, M., & Ramakrishna, S. (2003). A review on polymer nanofibers by electrospinning and their applications in nanocomposites. *Composites Science and Technology, 63*(15), 2223-2253. doi: 10.1016/S0266-3538(03)00178-7

[66] Thavasi, V., Singh, G., & Ramakrishna, S. (2008). Electrospun nanofibers in energy and environmental applications. *Energy & Environmental Science, 1*(2), 205. doi: 10.1039/b809074m

[67] Pham, Q. P., Sharma, U., & Mikos, A. G. (2006). Electrospinning of polymeric nanofibers for tissue engineering applications: A review. *Tissue Engineering,12*(5), 1197-1211. doi: 10.1089/ten.2006.12.1197

[68] Zong, X., Kim, K., Fang, D., Ran, S., Hsiao, B. S., & Chu, B. (2002). Structure and process relationship of electrospun bioabsorbable nanofiber membranes. *Polymer, 43*(16), 4403-4412. doi: 10.1016/S0032-3861(02)00275-6

[69] Deitzel, J. M., Kleinmeyer, J., Harris, D., & Beck Tan, N. C. (2001). The effect of processing variables on the morphology of electrospun nanofibers and textiles. *Polymer, 42*(1), 261-272. doi: 10.1016/S0032-3861(00)00250-0

[70] Park, J., Choi, J., Jo, S., Lim, Y., Gwon, H., Khil, M. S., & Nho, Y. (2012). Characterization and structure analysis of PLGA/collagen nanofibrous membranes by electrospinning.*Journal of Applied Polymer Science, 125*(S2), E595-E603. doi: 10.1002/app.36833

[71] Fong, H., Chun, I., & Reneker, D. H. (1999). Beaded nanofibers formed during electrospinning. *Polymer, 40*(16), 4585-4592. doi: 10.1016/S0032-3861(99)00068-3

[72] Geng, X., Kwon, O., & Jang, J. (2005). Electrospinning of chitosan dissolved in concentrated acetic acid solution.*Biomaterials, 26*(27), 5427-5432. doi: 10.1016/j.biomaterials.2005.01.066

[73] Study on wet-laid nonwoven separator of lithium-ion battery. (2012). Textile Research Journal, 82(16), 1659-1665. doi:10.1177/0040517511431314

[74] Casper, C. L., Stephens, J. S., Tassi, N. G., Chase, D. B., & Rabolt, J. F. (2004). Controlling surface morphology of electrospun polystyrene fibers: effect of humidity and molecular weight in the electrospinning process.*Macromolecules, 37*(2), 573-578. doi: 10.1021/ma0351975

[75] Koski, A., Yim, K., & Shivkumar, S. (2004). Effect of molecular weight on fibrous PVA produced by electrospinning. *Materials Letters, 58*(3), 493-497. doi: 10.1016/S0167-577X(03)00532-9

[76] Krigbaum, W. R., Mandelkern, L., & Flory, P. J. (1952). Molecular weight dependence of intrinsic viscosity of polymer solutions.*Journal of Polymer Science, 9*(4), 381-384. doi: 10.1002/pol.1952.120090408

[77] Lim, H. J., Lee, S. J., Bae, H. J., Noh, S. K., Lee, Y. R., Han, S. S., ... (2007). Effects of the tacticities of poly(vinyl alcohol) on the structure and morphology of poly(vinyl alcohol) nanowebs prepared by electrospinning. *Journal of Applied Polymer Science, 106*(5), 3282-3289. doi: 10.1002/app.26556

[78] Nie, H., He, A., Zheng, J., Xu, S., Li, J., & Han, C. C. (2008). Effects of chain conformation and entanglement on the electrospinning of pure alginate. *Biomacromolecules, 9*(5), 1362-1365. doi: 10.1021/bm701349j

[79] Miao, Y., Zhu, G., Hou, H., Xia, Y., & Liu, T. (2013). Electrospun polyimide

nanofiber-based nonwoven separators for lithium-ion batteries. *Journal of Power Sources, 226*, 82-86. doi: 10.1016/j.jpowsour.2012.10.027

[80] Sohn, J., Im, J., Shin, J., & Nho, Y. (2012). PVDF-HFP/PMMA-coated PE separator for lithium ion battery. *Journal of Solid State Electrochemistry, 16*(2), 551-556. doi: 10.1007/s10008-011-1379-7

[81] Sohn, J., Im, J. S., Gwon, S., Choi, J., Shin, J., & Nho, Y. (2009). Preparation and characterization of a PVDF-HFP/PEGDMA-coated PE separator for lithium-ion polymer battery by electron beam irradiation. *Radiation Physics and Chemistry, 78*(7), 505-508. doi: 10.1016/j.radphyschem.2009.03.035

[82] Lee, J. A., Lee, J. Y., Ryou, M. H., Han, G., Lee, J., Lee, D., . . . Lee, Y. M. (2011). Anion receptor-coated separator for lithium-ion polymer battery. *Journal of Solid State Electrochemistry, 15*(4), 753-757. doi: 10.1007/s10008-010-1149-y

[83] Kim, J. Y., Lee, Y., & Lim, D. Y. (2009). Plasma-modified polyethylene membrane as a separator for lithium-ion polymer battery. *Electrochimica Acta, 54*(14), 3714-3719. doi: 10.1016/j.electacta.2009.01.055

[84] Liang, Y., Lin, Z., Qiu, Y., & Zhang, X. (2011). Fabrication and characterization of LATP/PAN composite fiber-based lithium-ion battery separators. *Electrochimica Acta, 56*(18), 6474-6480. doi: 10.1016/j.electacta.2011.05.007

[85] Liang, Y., Ji, L., Guo, B., Lin, Z., Yao, Y., Li, Y., . . . Zhang, X. (2011). Preparation and electrochemical characterization of ionic-conducting lithium lanthanum titanate oxide/polyacrylonitrile submicron composite fiber-based lithium-ion battery separators.*Journal of Power Sources, 196*(1), 436-441. doi: 10.1016/j.jpowsour.2010.06.088

[86] Ding, Y., Zhang, P., Long, Z., Jiang, Y., Xu, F., & Di, W. (2009). The ionic conductivity and mechanical property of electrospun P(VdF-HFP)/PMMA membranes for lithium ion batteries. *Journal of Membrane Science, 329*(1), 56-59. doi: 10.1016/j.memsci.2008.12.024

[87] Zhang, S. S. (2007). A review on the separators of liquid electrolyte li-ion batteries. *Journal of Power Sources, 164*(1), 351-364. doi: 10.1016/j.jpowsour.2006.10.065

[88] Wang, G., Shen, X., Yao, J., & Park, J. (2009). Graphene nanosheets for enhanced lithium storage in lithium ion batteries.*Carbon, 47*(8), 2049-2053. doi: 10.1016/j.carbon.2009.03.053

[89] Yi, W., Huaiyu, Z., Jian, H., Yun, L., & Shushu, Z. (2009). Wet-laid non-woven fabric for separator of lithium-ion battery.*Journal of Power Sources, 189*(1), 616-619. doi: 10.1016/j.jpowsour.2008.09.078

[90] Venugopal, G., Moore, J., Howard, J., & Pendalwar, S. (1999). Characterization of microporous separators for lithium-ion batteries. *Journal of Power Sources, 77*(1), 34-41. doi: 10.1016/S0378-7753(98)00168-2

[91] Lee, Y. M., Lee, J. A., Choi, N., Seol, W., Cho, K., Jung, H., . . . Park, J. (2005). Electrochemical effect of coating layer on the separator based on PVdF and PE non-woven matrix. *Journal of Power Sources, 146*(1), 431-435. doi: 10.1016/j.jpowsour.2005.03.047

[92] Boudin, F., Andrieu, X., Jehoulet, C., & Olsen, I. I. (1999). Microporous PVdF gel for lithium-ion batteries. *Journal of Power Sources, 81*, 804-807. doi: 10.1016/S0378-7753(99)00154-8

[93] Ren, Z., Liu, Y., Sun, K., Zhou, X., & Zhang, N. (2009). A microporous gel electrolyte based on poly(vinylidene fluoride-co-hexafluoropropylene)/fully cyanoethylated cellulose derivative blend for lithium-ion battery. *Electrochimica Acta,54*(6), 1888-1892. doi: 10.1016/j.electacta.2008.10.011

[94] Kim, J. Y., & Lim, D. Y. (2010). Surface-modified membrane as A separator for lithium-ion polymer battery. *Energies, 3*(4), 866-885. doi: 10.3390/en3040866

[95] Kim, K. J., Kim, Y. H., Kim, J., Kim, Y., Song, J. H., & Jo, Y. N. (2010). Effect of gamma ray irradiation on thermal and electrochemical properties of polyethylene separator for li ion batteries. *Journal of Power Sources, 195*(18), 6075-6080. doi: 10.1016/j.jpowsour.2009.12.056

[96] Zhang, P., Zhang, H. P., Li, Z. H., Sun, M., Wu, H. Q., & Wu, Y. P. (2007). A novel sandwiched membrane as polymer electrolyte for lithium ion battery. *Electrochemistry Communications, 9*(7), 1700-1703. doi: 10.1016/j.elecom.2007.03.021

[97] Bolto, B., Tran, T., Hoang, M., & Xie, Z. (2009). Crosslinked poly(vinyl alcohol) membranes. *Progress in Polymer Science, 34*(9), 969-981. doi: 10.1016/j.progpolymsci.2009.05.003

[98] Neubert, S., Pliszka, D., Thavasi, V., Wintermantel, E., & Ramakrishna, S. (2011). Conductive electrospun PANi-PEO/TiO2 fibrous membrane for photo catalysis. *Materials Science and Engineering: B, 176*(8), 640-646. doi: 10.1016/j.mseb.2011.02.007

[99] Aliabadi, M., Irani, M., Ismaeili, J., Piri, H., & Parnian, M. J. (2013). Electrospun nanofiber membrane of PEO/Chitosan for the adsorption of nickel, cadmium, lead and copper ions from aqueous solution. *Chemical Engineering Journal, 220*, 237-243. doi: 10.1016/j.cej.2013.01.021

[100] Aussawasathien, D., Dong, J. -., & Dai, L. (2005). Electrospun polymer nanofiber sensors. *Synthetic Metals,154*(1), 37-40. doi: 10.1016/j.synthmet.2005.07.018

[101] Na, H., Zhao, Y., Liu, X., Zhao, C., & Yuan, X. (2011). Structure and properties of electrospun poly(vinylidene fluoride)/polycarbonate membranes after hot-press. *Journal of Applied Polymer Science, 122*(2), 774-781. doi: 10.1002/app.33964

[102] Feng, Y., Meng, F., Xiao, R., Zhao, H., & Guo, J. (2011). Electrospinning of polycarbonate urethane biomaterials.*Frontiers of Chemical Science and Engineering, 5*(1), 11-18. doi: 10.1007/s11705-010-1011-x

[103] Li, S., & Wu, W. (2009). Lipase-immobilized electrospun PAN nanofibrous membranes for soybean oil hydrolysis.*Biochemical Engineering Journal, 45*(1), 48-53. doi: 10.1016/j.bej.2009.02.004

[104] Yoon, K., Kim, K., Wang, X., Fang, D., Hsiao, B. S., & Chu, B. (2006). High flux ultrafiltration membranes based on electrospun nanofibrous PAN scaffolds and chitosan coating.*Polymer, 47*(7), 2434-2441. doi: 10.1016/j.polymer.2006.01.042

[105] Zhong, Z., Cao, Q., Wang, X., Wu, N., & Wang, Y. (2012). PVC–PMMA composite electrospun membranes as polymer electrolytes for polymer lithium-ion batteries. *Ionics, 18*(1), 47-53. doi: 10.1007/s11581-011-0615-6

[106] Ding, Y., Zhang, P., Long, Z., Jiang, Y., Xu, F., & Di, W. (2009). The ionic conductivity and mechanical property of electrospun P(VdF-HFP)/PMMA membranes for lithium ion batteries. *Journal of Membrane Science, 329*(1), 56-59. doi: 10.1016/j.memsci.2008.12.024

[107] Zhang, J., Yang, M., Maurer, F., Common departments, the faculties of Science and Engineering, Lund University, Gemensamma institutioner för naturvetenskapliga och tekniska fakulteterna, . . . Kemicentrum. (2011). Effect of TiO2 formation on the free volume properties of electrospun PMMA nanohybrids. *Macromolecules,*

[108] Gopalan, A. I., Santhosh, P., Manesh, K. M., Nho, J. H., Kim, S. H., Hwang, C., & Lee, K. (2008). Development of electrospun PVdF–PAN membrane-based polymer electrolytes for lithium batteries. *Journal of Membrane Science, 325*(2), 683-690. doi: 10.1016/j.memsci.2008.08.047

[109] Kim, Y., Ahn, C. H., & Choi, M. O. (2010). Effect of thermal treatment on the characteristics of electrospun PVDF−silica composite nanofibrous membrane. *European Polymer Journal,46*(10), 1957-1965. doi: 10.1016/j.eurpolymj.2010.08.009

[110] Cheng, S. C., Liang, Y. Z., & Qiu, Y. P. (2012). Effect of thermal treatment on the physical properties of electrospun PVDF membrane. *Advanced Materials Research, 591-593*, 1113-1116. doi: 10.4028/www.scientific.net/AMR.591-593.1113

[111] Hao, J., Lei, G., Li, Z., Wu, L., Xiao, Q., & Wang, L. (2013). A novel polyethylene terephthalate nonwoven separator based on electrospinning technique for lithium ion battery. *Journal of Membrane Science, 428*, 11-16. doi: 10.1016/j.memsci.2012.09.058

[112] Na, H., Zhao, Y., Zhao, C., Zhao, C., & Yuan, X. (2008). Effect of hot-press on electrospun poly(vinylidene fluoride) membranes. *Polymer Engineering & Science, 48*(5), 934-940. doi: 10.1002/pen.21039

[113] Kim, J. R., Kim, B. C., Choi, S. W., Jo, S. M., & Lee, W. S. (2004). Electrospun PVdF-based fibrous polymer electrolytes for lithium ion polymer batteries. *Electrochimica Acta, 50*(1), 69-75. doi: 10.1016/j.electacta.2004.07.014

[114] Abraham, K. M. (1993). Directions in secondary lithium battery research and development. *Electrochimica Acta, 38*(9), 1233-1248. doi: 10.1016/0013-4686(93)80054-4

[115] Li, X., Cheruvally, G., Kim, K., Kim, J., Choi, J., Ahn, H., & Ahn, J. (2007). Polymer electrolytes based on an electrospun poly(vinylidene fluoride-co-hexafluoropropylene) membrane for lithium batteries. *Journal of Power Sources, 167*(2), 491-498. doi: 10.1016/j.jpowsour.2007.02.032

[116] Jung, H., Ju, D., Lee, W., Zhang, X., & Kotek, R. (2009). Electrospun hydrophilic fumed silica/polyacrylonitrile nanofiber-based composite electrolyte membranes. *Electrochimica Acta,54*(13), 3630-3637. doi: 10.1016/j.electacta.2009.01.039

[117] Cheruvally, G., Song, C. E., Kim, K., Kim, J., Choi, J., Choi, D. S., . . . Raghavan, P. (2007). Electrospun polymer membrane activated with room temperature ionic liquid: Novel polymer electrolytes for lithium batteries. *Journal of Power Sources,172*(2), 863-869. doi: 10.1016/j.jpowsour.2007.07.057

[118] Kim, J. Y., Lee, Y., & Lim, D. Y. (2009). Plasma-modified polyethylene membrane as a separator for lithium-ion polymer battery. *Electrochimica Acta, 54*(14), 3714-3719. doi: 10.1016/j.electacta.2009.01.055

[119] Shin, W., & Kim, D. (2013). High performance ceramic-coated separators prepared with lithium ion-containing SiO2 particles for lithium-ion batteries. *Journal of Power Sources, 226*, 54-60. doi: 10.1016/j.jpowsour.2012.10.082